ALMOST GLOBAL FEEDBACK CONTROL OF AUTONOMOUS UNDERWATER VEHICLES

By

Shashi Bhushan Singh

Bachelor of Technology in Ocean Engineering and Naval Architecture

Indian Institute of Technology, Kharagpur, India

Submitted to the Department of Mathematics

in Partial Fulfillment of the Requirements of the Degree of

Master of Arts in Mathematics

at the

University of Hawaii, Manoa

December 2008

Thesis Committee:

Monique Chyba, Chairperson

Amit Kumar Sanyal

George R. Wilkens

We certify that we have read this document and that, in our opinion, it is satisfactory in scope and quality as a thesis for the degree of Master of Arts in Mathematics.

THESIS COMMITTEE

_____
Chairperson

_____

_____

_____

_____

_____

ALMOST GLOBAL FEEDBACK CONTROL OF AUTONOMOUS UNDERWATER VEHICLES

By

Shashi Bhushan Singh

Submitted to the Department of Mathematics on December 8,2008 in partial fulfillment of the requirements for the degree of Master of Arts in Mathematics.

Abstract

An Autonomous Underwater Vehicle (AUV) is expected to operate in an aquatic environment and compensate for poorly known disturbance forces and moments. Due to uncertain environment, it is difficult to apply an open-loop control scheme for tracking the desired trajectory. The objective of this thesis is to develop a robust feedback trajectory tracking control scheme for an AUV that can track a prescribed trajectory amidst such disturbances.

This thesis is composed of two parts. In the first part, we study the problem of attitude tracking of an AUV submerged in an ideal fluid. The feedback control scheme is a recently reported almost global tracking control scheme for attitude and angular velocity of a rigid body in the presence of external torques. The feedback-controlled attitude dynamics of the AUV is simulated and the results corroborate the expected almost global tracking behavior of the feedback system. In the second part, we solve a more general problem of tracking

both the orientation and position of the vehicle submerged in a real fluid. The feedback control scheme is derived using Lyapunov-type analysis. The results obtained from numerical simulations confirm the asymptotic tracking properties of the feedback control law. We apply the feedback control scheme for different mission scenarios of an AUV with an initial error in its states.

Am accurate and efficient numerical integration scheme is crucial to verify the controller performance in the closed-loop feedback dynamics. Employing an accurate computational approach which respects the geometry of the problem has been one of the focal points of this research. We use a Lie group variational integrator to simulate the feedback attitude dynamics of an AUV. Differential equations on a matrix Lie group that governs the closed loop kinematics is solved using the Crouch-Grossman (CG) method. The CG method coupled with a fourth-order Runge-Kutta method is used to simulate the feedback dynamics of the vehicle in $\mathrm{SE}(3)$.

Acknowledgments

I owe my thanks to my advisers, Professor Monique Chyba and Professor Amit Kumar Sanyal, who provided constant guidance, inspiration and support during the course of this work. Without their help, this thesis would have never seen the light of day. Working next to them for the past one and a half year has been an invaluable learning experience.

Many thanks to Professor George Wilkens for introducing me to the exciting world of geometric control theory. Also, I take this opportunity to thank Professor Lewis Bowen, Professor Ronald Brown, Professor Thomas Craven, Professor George Csordas, and Professor David Stegenga for helping an engineer discover the beauty of Mathematics.

I also express my gratitude towards the other faculty members. They have been a constant source of inspiration for me. I acknowledge the support that I have received from Pat, Shirley, Susan, and Troy. They have been very helpful and kind to me.

I owe my thanks to Ryan and Nikolaj for helping me in my research. Also I would like to thank my fellow students outside the department, Mukesh and Pranjal, for their constant support.

I am thankful to all the graduate students in this department for encouraging me in my academic pursuit. I am grateful for the creative interaction with my fellow students from this department: Xiongzhi Chen (Chee), Quinn Culver, Lukasz Grabarek, Ni Lu, and Vu

Nguyen. They have helped me solve problems and move on countless times.

I am indebted to my past teachers, colleagues, and friends who in countless ways contributed to my education. My parents have been with me constantly, albeit from a great distance. I would not have been able to accomplish much without their support. I thank my sisters for their love and support.

Shashi Bhushan Singh

Honolulu, 2008.

Contents

List of Figures

Chapter 1
Introduction

Oceans cover two-thirds of the earth and have a large influence on the global climate. They have a great impact on the lives of human beings, plants and animals. They are a huge source of mineral resources. However, many of these resources still remain untapped and potentially unknown.

With the advancement of technology, man has stepped on moon. Several unmanned missions have been carried out successfully to the outer reaches of space. Scientists have been successful in sending robots to as far as Mars. However, planning a successful voyage to the abyssal world still remains elusive for researchers.

Executing a manned voyage to the deep sea is extremely risky because of the unknown environment. Moreover, the oceanic environment is not ideal for humans, as the ambient pressure is unbearable at depths as shallow as 200m. Thus unmanned underwater robots prove to be an ideal platform to perform deep sea research.

Underwater robots can help us in many ways to understand the effect that oceans have on our climate. They can be utilized in geological and oceanographic research. Furthermore, they are instrumental in exploring vast ocean resources which can be used for the welfare of mankind. They can prove to be a huge asset to the oil industries in ocean-bed survey and resource assessment. They can also be utilized for military purposes such as shallow water mine search and disposal. Moreover, they can be employed for doing ship-hull inspection and numerous other works related to marine industry. Thus, it is evident

that the development in underwater research has vast social, economic and military implications.

A successful execution of all of the above missions and several others, requires robust control of the motion of the underwater vehicle. The primary difficulty in their control is because of their non-linear dynamics (see [3]). The hydrodynamic parameters governing the dynamics are highly nonlinear, coupled and time varying. Unlike terrestrial or aerial vehicles, underwater vehicles can not use Global Positioning System (GPS). Sonar based sensors are the commonly used underwater sensors. But their measurements are usually crippled by noise, missed detection, poor resolution, etc. Thus the state-of-the-art underwater robotic technologies need further development.

In the next section, we do a brief overview on the research and development in underwater robotics over the last two decades.

1.1 Control of Underwater Vehicles: A Brief Survey

Until recently, remotely operated vehicles (ROVs) have been used as a platform for underwater robot manipulators [19], [20], [54]- [58]. As the name suggests, ROVs are underwater vehicles controlled by operators aboard a ship or at shore. The transmission of electrical signals back and forth between the operator and the vehicle is made via group of cables attached to the vehicle. However, the cables limits the maneuverability of the vehicle and puts constraints on depth. Also, because of operator fatigue and limited area of operation, extensive use of tethered ROVs is limited to a few specific applications, such as

shallow water oceanogrphic data collection. Thus with the increasing demand for imparting greater autonomy to underwater vehicles, researchers around the world are focusing on developing intelligent, decision-making AUV. References related to the research on AUVs can be found in [2], [10]- [14], [24], [28], [31], [38], [50], [51] and the references contained therein.

A detailed survey on the research and development in the control of underwater robots in the 1990s can be found in [59]. It gives a detailed survey on some key areas on the existent state-of-the-art underwater technologies. It also gives a comprehensive list of a worldwide development of AUVs, their configurations and their specific mission requirements during that period.

Researchers have proposed numerous advanced controllers for underwater vehicles. In the next section, we provide a literature survey on various controllers that have been successfully implemented on underwater vehicles.

1.1.1 Proportional-Integral-Derivative Control

A Propotional-Integral-Derivative (PID) control design takes into account error in the current state as compared to the desired state, sum of previous errors and the rate of change of error. In [54], the authors used a PID controller for their vehicle, an ROV. A PID-based control technique for the navigation control system of an AUV is reported in [28].

1.1.2 Sliding Mode Control

Sliding mode control has been applied successfully in the control of underwater vehicles in [56, 57]. The control scheme involves twin tasks of selection of a manifold such that the system trajectory exhibits desirable behavior when confined to this manifold, and finding feedback gains so that the system trajectory intersects and stays on the manifold. For a thorough knowledge on differential geometric concepts we direct our reader to [5]. In [58], the authors discuss how adaptive sliding control can be applied to underwater vehicles. In [16], an adaptive sliding mode controller is applied to control an AUV in the dive plane. The use of multi-variable sliding mode controller for autonomous diving and steering of unmanned underwater vehicles is reported in [24]. Sliding mode control can lead to chattering which must be eliminated in order for the controller to perform properly.

Because of their nonlinear dynamics, uncertain models and the presence of underestimated, often unestimated, disturbances there is always a need for designing an improved robust controller for underwater vehicles. In [57], the authors have developed an extension of sliding mode control which is robust to imprecise models and which explicitly accounts for the presence of high-frequency unmodeled dynamics.

1.1.3 $\mathscr{H}_\infty$ Control

An $\mathscr{H}_\infty$ type control is an optimal control design technique which is robust to process and measurement noise. This control addresses the problem of robustness by deriving controllers which maintain system response and error signals to within prescribed tolerances, despite the presence of noise in the system. Applications of such controller to the control of submarines has been reported in [41, 53, 55]. In [29], the authors have designed a multiple-input-multiple-output (MIMO) controller for an AUV using standard techniques of $\mathscr{H}_\infty$ theory.

1.1.4 Adaptive Control

In robotics, adaptive controllers have been shown to give high performance for nonlinear systems [15, 45, 49, 52]. When designing controllers for underwater robotic systems, it is necessary to compensate for model features such as nonlinear dynamics, uncertain and time-varying parameters. This suggests a robust adaptive control scheme for an underwater vehicle. An adaptive control changes the control law used by the controller to adapt to the changing parameters. Application of adaptive control to underwater vehicles has been documented in [2, 58, 60, 61, 63].

1.1.5 Control Using Fuzzy Logic, Neural Network and Genetic Algorithm Techniques

Tools such as fuzzy logic (see [62]), neural networks and genetic algorithms have also been applied by various researchers in robotic control. Often times these are combined together to design a robust control scheme by deriving advantages from each of the individual components. In [31], the authors have studied the application of neuro-fuzzy controller for AUVs. An adaptive neural-net controller system for an underwater vehicle has been designed in [27]. A self-adaptive neuro-fuzzy system with fast parameter learning for AUVs has been reported in [33].

1.1.6 Geometric Control

During the past decade, a number of researchers have dealt with the problem of control of AUVs using a differential geometric architecture. We must note that the present research has been undertaken in the same spirit. One of the reasons for choosing this approach is that the configurations defined by a rigid body correspond naturally to a differentiable manifold in a one to one manner. This allows us to work with the actual structure of the problem, without being trapped in the complications associated with a certain choice of coordinates while representing the dynamics of a rigid body. One can derive motivation for this approach from [40].

We would find [7] very helpful in understanding the modeling and control of mechanical systems using a geometric framework. Applications of geometric control to AUVs can be found in [12, 13, 14, 36, 37, 50]. Moreover in [10, 11], the authors have investigated the design and implementation of time efficient and energy efficient trajectories for an AUV using geometric control. Research has also been undertaken in the area of control of *underactuated* AUVs, i.e. the vehicle loses direct control on one or more degrees of freedom. A sample of such work can be found in [38, 39, 50, 51].

1.2 Overall Layout

In Chapter 2, we state the feedback control problems that are solved in this thesis. Chapter 3 presents a model of the dynamics of a submerged rigid body. We briefly discuss the various forces and moments that act on a body moving in a viscous fluid. In chapter 4, we give the feedback control approach for the attitude tracking of a rigid body submerged in an ideal fluid. Chapter 5 formulates the feedback tracking problem of a submerged rigid body in the state-space $\mathrm{TSE}(3)$. In Chapter 6, we briefly discuss the Lyapunov analysis done for deriving the feedback control scheme. Chapter 7 discusses the application of a kinematic reduction and use of decoupling vector fields for designing the reference trajectory to be tracked by the controller. We discuss the various integration schemes used for our simulations in Chapter 8. In Chapters 9 and 10, we present the simulation results for the trajectory tracking in $\mathrm{SO}(3)$ and $\mathrm{SE}(3)$ respectively. Chapter 11 discusses possible future work.

Chapter 2
Problem Statement

This work is mainly focused on the challenging problem of trajectory tracking for an AUV in the presence of poorly known disturbance forces and moments. However, the theory can also be applied to the trajectory tracking of a remotely-operated aerial or underwater vehicle. In Chapter 1 we mentioned that the hydrodynamic parameters which influence the dynamics of the vehicle are highly nonlinear and time varying. Applying an open-loop control to perform a desired task is not possible in such cases. In such cases one can not apply a corrective force or moment to compensate for the error caused by unmodeled disturbances. A slight change in the state of the vehicle at the start of its mission could lead to a large final error in its state.

An open-loop, optimal control scheme for the motion planning of a test bed AUV has been reported to be designed and implemented in [10, 11]. In [13, 50, 51], the authors have successfully implemented an open-loop motion planning algorithm, derived using a kinematic reduction and decoupling vector fields, on a test-bed AUV. However, it should be noted that all these experiments were carried out in a controlled environment where the disturbance forces are negligible.

In a real-world application, an AUV has to account for the dynamic environment of the ocean. While in the ocean, an AUV experiences forces and moments which are very uncertain and hence can not be modeled accurately. Amidst such an environment, the missions implemented using open-loop control strategies can not be strictly realized. Therefore in

such cases, a feedback trajectory tracking control scheme that is robust to these disturbances would be essential to ensure that the vehicle tracks the desired trajectory.

2.1 Feedback Trajectory Tracking in $\mathrm{SO}(3)$

To better understand the trajectory tracking problem for an AUV in $\mathrm{SE}(3)$, we first consider the attitude tracking problem in $\mathrm{SO}(3)$. This problem refers to the feedback control of the attitude dynamics of an AUV. The attitude of any rigid body is defined as the relative orientation of a body-fixed coordinate frame to an inertial frame. It is represented globally by a group of special orthogonal matrices, $\mathrm{SO}(3)$. Trajectory tracking in $\mathrm{SO}(3)$ finds its application in spacecraft control, control of aerospace and underwater vehicles, control of mobile robots, and networked control of such autonomous systems.

The dynamics of a feedback-controlled rigid body system evolves on $\mathrm{TSO}(3)$. Recent research, reported in [9, 46, 47], has been successful in demonstrating almost global trajectory tracking in $\mathrm{TSO}(3)$, applied to spacecraft control. The almost global property of the control scheme refers to the fact that a desired attitude or attitude motion trajectory may be obtained starting from almost any initial state, modulo a set of measure zero, in the state space $\mathrm{TSO}(3)$. In [46], the authors have included the effects of additional disturbance moments (bounded but unknown) on the attitude dynamics, and demonstrated that the desired trajectory in $\mathrm{TSO}(3)$ could be tracked satisfactorily and almost globally, even in the presence of such disturbances. In Chapter 4, we will consider the problem of attitude tracking of an AUV submerged in an ideal fluid under the assumption that the translational

velocity is zero, and the moment due to external disturbances is absent.

2.2 Feedback Trajectory Tracking in $\mathrm{SE}(3)$

Trajectory tracking of an AUV in $\mathrm{SE}(3)$ is an extension of the attitude tracking problem in $\mathrm{SO}(3)$; the extension includes the translational motion in its dynamics. The addition of translational motion introduces dynamic coupling between the attitude and translational degrees of freedom (DOF). This coupling is very strong in an AUV, since the energy distributed among the translational DOF is comparable to the energy in the attitude DOF. This is unlike a spacecraft or aerial vehicle, where translational DOF have more energy than the rotational (attitude) DOF. In Chapter 5, we investigate an almost global asymptotic trajectory tracking of reference trajectories of an AUV in $\mathrm{TSE}(3)$, in the absence of disturbance inputs. The reference trajectories are taken from different mission scenarios reported in [50]. Here the author implemented an open-loop motion planning algorithm on the test-bed AUV, called ODIN[1].

[1]The Omni-Directional Intelligent Navigator (ODIN) is owned and maintained by Autonomous Systems Laboratory (ASL), College of Engineering, University of Hawaii, Manoa

2.3 Structure-Preserving Numerical Integration Scheme

In addition to designing the control scheme for the trajectory tracking problem at hand, a major focus of this research has been on employing efficient and accurate computational approaches which respect the geometry of the problem. Numerical methods that preserve the geometric properties have been studied in [23]. In our current research, we will be implementing such structure-preserving integration schemes that maintain the structure of the configuration space (see Chapter 8). An example of such a scheme is the Crouch-Grossmann integrator for attitude motion (see [18, 23]), coupled with the fourth-order Runge-Kutta scheme for translational motion. We will be using this numerical scheme for simulating the feedback trajectory tracking in $\mathrm{SE}(3)$.

A Lie group variational integrator is another example of a structure preserving numerical integrator. This variational integrator exhibits symplectic and momentum preserving properties, as well as good energy behavior characteristics of variational integrators (see [23, 42]). This class of variational integrators has been reported to be used in [34, 35, 48] for the attitude dynamics of a rigid body. We use this Lie group variational integrator to numerically simulate the feedback tracking in $\mathrm{SO}(3)$. A Lie group variational integrator for motion in $\mathrm{SE}(3)$ has been developed in [35]. However, we will not be using it in this thesis.

Chapter 3
Modeling the Dynamics of an AUV

In the present work we express the dynamics of a submerged rigid body in the framework of geometric mechanics. Since coordinates are only valid for a local region of a configuration space, by looking at the dynamics in a coordinate frame we loose the inherent global properties of the mechanical system and its manifold structure. The dynamics expressed in coordinate invariant setting allows us to describe the motion of a rigid body in a global setting and thus preserve the structure of the problem. We model the dynamics of an AUV by use of ideas from [7, 50].

We begin by describing the kinematic equations for a rigid body. Next, we discuss the hydrodynamic forces and moments that act upon the body when submerged in fluid. A proper understanding of these forces is crucial to understand the underlying dynamics of an AUV moving in a viscous fluid. Following this, we obtain the dynamics governing the motion of an AUV in a real fluid in a geometric setting. At the end, we provide a coordinate representation of these kinematic and dynamic equations. We also note here that the phrase *submerged rigid body* has different meanings when used in different contexts. In this thesis, we will use AUV and submerged rigid body interchangeably.

3.1 Model of AUV Kinematics

The position and orientation of an AUV at any point in time can be represented by (b, R), where $b \in \mathbb{R}^3$ and $R \in \mathrm{SO}(3)$ is a rotation matrix. In the above notation, b gives the position of the origin of a body-fixed frame O_B, with respect to the origin of an inertial frame O_I. The rotation matrix R,gives the attitude of a rigid body. We define R to be the matrix that when multiplied by a vector expressed in a body-fixed frame yields the same vector expressed in the inertial frame. That is, if $z \in \mathbb{R}^3$ is a vector in the inertial frame and $z' \in \mathbb{R}^3$ is the same vector expressed in the body-frame, then $z = Rz'$.

We can write the rotation matrix in terms of the Euler angles: ϕ, θ and ψ. The rotation about the x-axis (roll) is denoted by ϕ, rotation about the y-axis (pitch) is given by θ, and the rotation about the z-axis (yaw) is given by ψ. Using $(1, 2, 3)$ or (x, y, z) convention for Euler angles, the rotation matrix is represented as

$$R = \begin{bmatrix} c_\theta c_\psi & s_\phi s_\theta c_\psi - c_\phi s_\psi & c_\phi s_\theta c_\psi + s_\phi s_\psi \\ c_\theta s_\psi & s_\phi s_\theta s_\psi + c_\phi c_\psi & c_\phi s_\theta s_\psi - s_\phi c_\psi \\ -s_\theta & c_\theta s_\phi & c_\theta c_\phi \end{bmatrix},$$

where $c_\alpha = \cos(\alpha)$ and $s_\alpha = \sin(\alpha)$.

The configuration space of a rigid body is $\mathrm{SE}(3)$, the special Euclidean group. The Lie group $\mathrm{SE}(3)$ is the semi-direct product of $\mathrm{SO}(3)$ and $\mathbb{R}^3$. We denote the translational and

angular velocities in the body-fixed frame by ν and Ω, respectively. The kinematics of a rigid body are given by

$$\begin{aligned} \dot{b} &= R\nu \\ \dot{R} &= R\Omega^{\times}, \end{aligned} \tag{3.1}$$

where the operator $(\cdot)^{\times} : \mathbb{R}^3 \to \mathfrak{so}(3)$ is defined by $y^{\times}z = y \times z$. The space $\mathfrak{so}(3)$ is the Lie algebra of the Lie group $\mathrm{SO}(3)$, and is identified with the space of skew-symmetric 3×3 matrices.

3.2 Hydrodynamic Forces and Moments

It is an indispensable part of AUV research that we understand the environment that we are dealing with, and know the forces and moments acting on the vehicle due to its submersion in a viscous fluid. Thus, before we give the dynamic equations governing the motion of a submerged rigid body, let us analyze the hydrodynamic forces and moments that act on a submerged rigid body. A thorough treatment of the hydrodynamic forces and moments acting on a submerged rigid body can be obtained from [21, 32]. We first consider the restoring forces acting on an AUV. Next, we discuss the added mass forces and moments due to the inertia of the surrounding fluid. Finally, we discuss the dissipative forces acting on a body submerged in a viscous fluid. A detailed treatise on these forces and moments in both classical and geometric setting can be found in [50].

3.2.1 Restoring Forces and Moments

In hydrodynamic terminology, the forces and moments due to gravity and buoyancy are called restoring forces and moments. They are also called potential forces and moments. These forces and moments are conservative in nature. The gravitational force acts through the center of gravity $r_{C_g} = (x_G, y_G, z_G)$, whereas the buoyant force acts through the center of buoyancy $r_{C_B} = (x_B, y_B, z_B)$. Here, $r_{C_g}(r_{C_B})$ is the vector from the origin of the body-fixed frame of an AUV to its center of gravity, C_G (center of buoyancy C_B). The restoring force is given by $\boldsymbol{f}_g + \boldsymbol{f}_b$, where $\boldsymbol{f}_g$ is the gravitational force and $\boldsymbol{f}_b$ is the buoyant force. The restoring moment is given by $r_{C_G} \times \boldsymbol{f}_g + r_{C_B} \times \boldsymbol{f}_b$. Throughout this thesis, we will assume that $C_G = O_B, i.e.\ r_{C_G} = (0, 0, 0)^T$. Under this assumption the restroing moment reducess to $r_{C_B} \times \boldsymbol{f}_b$.

3.2.2 Added Mass Forces and Moments

According to [3], a body having an accelerated motion in a continuous medium of fluid experiences a force that is greater than the mass of the body times the acceleration. Since the increment of force can be defined as the product of the body acceleration and a quantity having the same dimension as mass, it is termed as added mass. However, one should remember that the concept of added mass is introduced into fluid mechanics for convenience of evaluation, and does not have any physical significance. For example, one should not

imagine that a body accelerating in an ideal fluid in a certain direction drags with it a certain amount of fluid mass.

According to fluid mechanics, the added mass forces and moments acting on a vehicle are pressure-induced forces and moments due to the inertia of the surrounding fluid and which are proportional to the acceleration of the body. In general, for a body performing movements in six DOF, the added mass is a 6×6 matrix called the added inertia matrix. Under the assumption of a low speed maneuver, which is quite normal in AUV applications, and three planes of symmetry in the vehicle design, the added inertia matrix can be reduced to a diagonal form. With these assumptions along with the added assumption that $C_G = O_B$, the added inertia matrix is given by

$$\begin{pmatrix} M_f^\nu & 0_{3\times3} \\ 0_{3\times3} & J_f^\Omega \end{pmatrix},$$

where $M_f^\nu = \text{diag}(M_f^{\nu_1}, M_f^{\nu_2}, M_f^{\nu_3})$ and $J_f^\Omega = \text{diag}(J_f^{\Omega_1}, J_f^{\Omega_2}, J_f^{\Omega_3})$ correspond to the translational forces and rotational moments, respectively (see [50]).

3.2.3 Hydrodynamic Damping

Hydrodynamic damping forces and moments are dissipative in nature and oppose the relative motion of the vehicle. Hydrodynamic damping can be caused by various factors, viz. radiation-induced potential due to forced body oscillations, linear or quadratic skin friction depending upon laminar or turbulent boundary layers respectively, wave drift damping and damping due to vortex shedding. A detailed description of the hydrodynamic damping forces acting on an underwater vehicle is given in [1].

The hydrodynamic damping of an underwater vehicle moving in 6 DOF at high speed will be highly nonlinear and coupled. Nevertheless, for our application, considering the spherical shape of the vehicle and its size, one can roughly estimate the drag forces and moments by assuming that the vehicle has three planes of symmetry and is performing non-coupled motions at low speed. For an AUV performing non-coupled motion at a slow speed, the drag matrix $D(\nu, \Omega)$ attains diagonal structure which is given by

$$D(\nu,\Omega) = \text{diag}(D_1(\nu)|\nu_1|, D_2(\nu)|\nu_2|, D_3(\nu)|\nu_3|, D_4(\Omega)|\Omega_1|, D_5(\Omega)|\Omega_2|, D_6(\Omega)|\Omega_3|),$$

where the D_i's are drag coefficients for the i^{th} direction of the velocity (see [50]). The drag effects depend on the velocity and the form (shape) of the vehicle.

In addition to the hydrodynamic forces discussed above, there are other forces which affect the dynamics of an AUV when it is moving underwater. For example, previous research (see [19, 20]) shows the drag effects of a communication cable attached to an underwater vehicle on its dynamics. The underwater vehicle that we use for our research is fully autonomous. However, we carry out control experiments in tethered mode so that we can perform multiple experiments for a single motion. We have studied the effect of umbilical cable on the dynamics of our test-bed AUV. The findings on the effect of various configurations of the cable attached to the vehicle have been reported in [11, 50]. The magnitude of these forces and moments are very small as compared to the forces and moments discussed above, so they are not included in the dynamic model.

3.3 Model of AUV Dynamics

Knowing all the external forces and moments acting on an AUV submerged in a viscous fluid, we are now ready to discuss the dynamic equations governing the motion of an AUV. Again, we should note that the dynamic equations of motion, discussed next, are developed in a differential geometric setting. In this setting the notion of acceleration and force is different from what one encounters in Newtonian mechanics. For a thorough investigation on this topic, see [7].

A detailed derivation of the dynamic equation of a rigid body submerged in a viscous fluid in the framework of geometric mechanics can be found in [50]. In the present work, we just state the governing equations.

Since $r_{C_G} = [0 \quad 0 \quad 0]^T$, the only moment due to the restoring buoyant force is the righting moment $-r_{C_B} \times (\rho g \mathcal{V}) R^T e_3$, where g is the acceleration due to gravity, $\mathcal{V}$ is the volume of the displaced fluid, and $e_3 = [0 \quad 0 \quad 1]^T$ is the inertial unit vector pointing in the direction of gravity. Let $e_1 = [1 \quad 0 \quad 0]^T$ and $e_2 = [0 \quad 1 \quad 0]^T$ denote the other unit vectors in the inertial frame such that $e_1, e_2,$ and e_3 form an orthonormal basis. The dynamic equations of motions are

$$\begin{aligned} M\dot{\nu} &= M\nu \times \Omega + D_\nu(\nu)\nu + (W - \rho g \mathcal{V}) R^T e_3 + \varphi_\nu + \varphi_\nu^d, \\ J\dot{\Omega} &= J\Omega \times \Omega + M\nu \times \nu + D_\Omega(\Omega)\Omega - r_{C_B} \times (\rho g \mathcal{V}) R^T e_3 + \tau_\Omega + \tau_\Omega^d, \text{ where} \end{aligned} \tag{3.2}$$

$D_\nu(\nu)\nu = \big(\text{diag}(D_1|\nu_1|, D_2|\nu_2|, D_3|\nu_3|)\big)\nu$ and $D_\Omega(\Omega)\Omega = \big(\text{diag}(D_4|\Omega_1|, D_5|\Omega_2|, D_6|\Omega_3|)\big)\Omega$ represent the drag force and drag momentum, respectively. Here, W is the weight of the AUV in air. The equations of motion are given by the kinematics (3.1) and the dynamics (3.2). The mass matrix $M = m\mathbb{I}_3 + M_f^\nu$ accounts for the mass and added mass, whereas the moment of inertia matrix $J = J_b + J_f^\Omega$ accounts for the body moments of inertia and the added mass moment of inertia. The vectors $\varphi_\nu^d \in \mathbb{R}^3$ and $\tau_\Omega^d \in \mathbb{R}^3$ are the bounded disturbance force and disturbance moment respectively, which we assume to be zero throughout this thesis. The control forces and moments of the AUV are given by $\varphi_\nu = (\varphi_{\nu_1}, \varphi_{\nu_2}, \varphi_{\nu_3})^T$ and $\tau_\Omega = (\tau_{\Omega_1}, \tau_{\Omega_2}, \tau_{\Omega_3})^T$, respectively.

Lemma 3.1. *The equations of motion expressed in coordinates of the body-fixed frame for a rigid body submerged in a viscous fluid subject to external forces are given by the following affine control system (see [10])*

$$\dot{b_1} = \nu_1 \cos\psi \cos\theta + \nu_2 R^{12} + \nu_3 R^{13}, \tag{3.3}$$

$$\dot{b_2} = \nu_2 \sin\psi \cos\theta + \nu_2 R^{22} + \nu_3 R^{23}, \tag{3.4}$$

$$\dot{b_3} = -\nu_1 \sin\theta + \nu_2 \cos\theta \sin\phi + \nu_3 \cos\theta \cos\phi, \tag{3.5}$$

$$\dot{\phi} = \Omega_1 + \Omega_2 \sin\phi \tan\theta + \Omega_3 \cos\phi \tan\theta, \tag{3.6}$$

$$\dot{\theta} = \Omega_2 \cos\phi - \Omega_3 \sin\phi, \tag{3.7}$$

$$\dot{\psi} = \frac{\sin\phi}{\cos\theta}\Omega_2 + \frac{\cos\phi}{\cos\theta}\Omega_3, \tag{3.8}$$

$$\dot{\nu_1} = \frac{1}{m_1}[-(m_3)\nu_3\Omega_2 + (m_2)\nu_2\Omega_3 + D_\nu(\nu_1) - G\sin\theta + \varphi_{\nu_1}], \tag{3.9}$$

$$\dot{\nu_2} = \frac{1}{m_2}[(m_3)\nu_3\Omega_1 - (m_1)\nu_1\Omega_3 + D_\nu(\nu_2) + G\cos\theta\sin\phi + \varphi_{\nu_2}], \tag{3.10}$$

$$\dot{\nu_3} = \frac{1}{m_3}[-(m_2)\nu_2\Omega_1 + (m_1)\nu_1\Omega_2 + D_\nu(\nu_3) + G\cos\theta\cos\phi + \varphi_{\nu_3}], \tag{3.11}$$

$$\tag{3.12}$$

$$\begin{aligned}\dot{\Omega_1} =& \frac{1}{J_{b_1} + J_f^{\Omega_1}}[(J_{b_2} - J_{b_3} + J_f^{\Omega_2} - J_f^{\Omega_3})\Omega_2\Omega_3 + (M_f^{\nu_2} - M_f^{\nu_3})\nu_2\nu_3 \\ &+ D_\Omega(\Omega_1) + \rho g\mathcal{V}(-y_B\cos\theta\cos\phi + z_B\cos\theta\sin\phi) + \tau_{\Omega_1}],\end{aligned} \tag{3.13}$$

$$\begin{aligned}\dot{\Omega_2} =& \frac{1}{J_{b_2} + J_f^{\Omega_2}}[(J_{b_3} - J_{b_1} + J_f^{\Omega_3} - J_f^{\Omega_1})\Omega_1\Omega_3 + (M_f^{\nu_3} - M_f^{\nu_1})\nu_1\nu_3 \\ &+ D_\Omega(\Omega_2) + \rho g\mathcal{V}(z_B\sin\theta + x_B\cos\theta\cos\phi) + \tau_{\Omega_2}],\end{aligned} \tag{3.14}$$

$$\begin{aligned}\dot{\Omega_3} =& \frac{1}{J_{b_3} + J_f^{\Omega_3}}[(J_{b_1} - J_{b_2} + J_f^{\Omega_1} - J_f^{\Omega_2})\Omega_1\Omega_2 + (M_f^{\nu_1} - M_f^{\nu_2})\nu_1\nu_2 \\ &+ D_\Omega(\Omega_3) + \rho g\mathcal{V}(-x_B\cos\theta\sin\phi - y_B\sin\theta) + \tau_{\Omega_3}],\end{aligned} \tag{3.15}$$

where $G = mg - \rho g\mathcal{V}, m_i = m + M_f^{\nu_i}, D_\nu(\nu_i) = D_i|\nu_i|, D_\Omega(\Omega_i) = D_{i+1}|\Omega_i|$ *where* $i = 1, 2, 3$. *Note that* $\varphi_\nu^d = \tau_\Omega^d = 0$. *Also,* $R^{12} = -\sin\psi\cos\phi + \cos\psi\sin\theta\sin\phi, R^{13} = \sin\psi\sin\phi + \cos\psi\cos\phi + \sin\phi\sin\theta\sin\psi, R^{22} = \cos\psi\cos\phi + \sin\phi\sin\theta\sin\psi,$ *and* $R^{23} = -\cos\psi\sin\phi + \sin\psi\cos\phi\sin\theta$.

Chapter 4
Almost Global Attitude Tracking of an AUV

The attitude of a rigid body is the relative orientation of the body-fixed coordinate frame to the inertial frame. The coordinate axes of these frames are related by a linear transformation given by a proper orthogonal matrix, called the rotation matrix. The rotation matrix can also be represented by coordinate sets, like the Euler angles or quaternions [21, 22]. We represent the global attitude by $R \in \mathrm{SO}(3)$, as mentioned in Section 3.1.

Before going any further, let us discuss some definitions and theorems which will be helpful in understanding the derivation of the feedback control law. The proofs of these can be found in [30].

Definition 4.1. An equilibrium point $x = 0 \in U \subset \mathbb{R}^n$ of a nonlinear system described by: $\dot{x} = f(x(t), t), x(t_0) = x_0$, where $x \in U$ and $f : U \times \mathbb{R} \to \mathbb{R}^n$ is a vector field, is

1. stable (in the sense of Lyapunov), if for all $t_0 \geq 0$ and $\epsilon > 0$, there exists a $\delta(t_0, \epsilon)$ such that $\|x_0\| < \delta(t_0, \epsilon) \Rightarrow \|x(t)\| < \epsilon, \forall t \geq t_0$. Here $x(t)$ is the solution of the nonlinear system.

2. unstable if it is not stable.

3. asymptotically stable if it is stable and attractive, i.e., for all $t_0 \geq 0$ there is a $\delta(t_0)$ such that $\|x_0\| < \delta \Rightarrow \lim_{t\to\infty} \|x(t)\| = 0$.

4. uniformly stable, if δ is chosen independent of t_0.

Theorem 4.1. *(Lyapunov Stability of Autonomous Systems) Let $x = 0$ be an equilibrium point for a system described by: $\dot{x} = f(x(t), t)$, where $f : U \to \mathbb{R}^n$ is locally Lipschitz and $U \subset \mathbb{R}^n$ is a domain that contains the origin. Let $V : U \to \mathbb{R}$ be a continuously differentiable, positive definite function in U.*

1. *If $\dot{V}(x) = [\partial V/\partial x]f$ is negative semidefinite, then $x = 0$ is a stable equilibrium point.*

2. *If $\dot{V}(x)$ is negative definite, then $x = 0$ is an asymptotically stable equilibrium point.*

In both cases above V is called a Lyapunov function. Moreover, if the conditions hold for all $x \in \mathbb{R}^n$ and $\|x\| \to \infty$, then $x = 0$ is globally stable in the first case and globally asymptotically stable in the second case.

Theorem 4.2. *(Lyapunov Uniform Asymptotically Stability of Non-Autonomous Systems) Let $x = 0$ be an equilibrium point of a system described by $\dot{x} = f(x, t)$ such that $x \in U \subset \mathbb{R}^n$, where U is a domain. Let $V : U \times [0, \infty] \to \mathbb{R}$ be a continuously differentiable function that satisfies*

$$W_1(x) \leq V(x, t) \leq W_2(x), \tag{4.1}$$

$$\dot{V}(x, t) = \frac{\partial V}{\partial t} + \frac{\partial V}{\partial x} f(x, t) \leq -W_3(x), \tag{4.2}$$

for all $t \geq t_0$, and $x \in U$, where $W_1(x), W_2(x)$ and $W_3(x)$ are continuous positive definite functions on U. Then, $x = 0$ is uniformly asymptotically stable and V is called a Lyapunov function. Furthermore, if $W_3(x) = 0$, then $x = 0$ is uniformly stable.

Corollary 4.1. *Suppose that the assumptions of Theorem 4.2 hold for all* $x \in \mathbb{R}^n$ *and* $W_1(x) \to \infty$ *for* $\|x\| \to \infty$, *then* $x = 0$ *is globally-uniformly-asymptotically stable.*

We will be applying the above concepts to obtain the feedback control scheme for the attitude tracking problem by doing Lyapunov-type analysis. In [9, 46] the authors have shown that such an analysis gives multiple critical points (at least four) for a feedback-controlled rigid body on $\mathrm{SO}(3)$. The stable manifolds of the non-minimum critical points are locally attractive, and this leads to loss of global-asymptotic stability. Nevertheless, using such a scheme leads to convergence of tracking errors for almost all initial conditions except those that lie on a set of measure zero (see [47]).

4.1 Modeling the Attitude Dynamics

The attitude tracking of a rigid body can be studied under various scenarios. In our case, we study the pure attitude motion of an AUV without any translation of its center of mass. Therefore, the translational velocity ν is assumed to be zero. Thus, from (3.1), the attitude kinematics equation can be given by $\dot{R} = R\Omega^{\times}$.

For the attitude tracking problem, we neglect the drag moment and any other external disturbance moments appearing in the dynamic equation given by Eq. (3.2). The assumption of zero drag moment essentially means that the AUV is moving in a perfect fluid, i.e., an inviscid and incompressible fluid. This assumption is not practical, as water is not a perfect fluid. However, we must note that the previous assumptions have been made as an

initial study of the use of the structure-preserving Lie group variational integrator to simulate the attitude feedback dynamics of an AUV. The use of the variational integrator in the presence of drag moments have been reported in [46], where the authors have investigated the disturbance- rejecting and feedback-tracking control of an spacecraft.

The attitude dynamic equations are obtained from (3.2) as

$$J\dot{\Omega} = J\Omega \times \Omega - r_{C_B} \times (\rho g \mathcal{V}) R^T e_3 + \tau, \tag{4.3}$$

where τ is the control input torque vector.

4.2 Modeling the Attitude Error Dynamics

In this section, we introduce the attitude and angular velocity trajectory tracking problem, and formulate it in terms of tracking errors in attitude and angular velocity. The reference trajectory is given by the initial attitude $R_r(0)$, and the angular velocity as a function of time $\Omega_r(t)$, for some interval of time $t \in [0, T]$, where $T > 0$. The reference angular velocity and acceleration, Ω_r and $\dot{\Omega}_r$, respectively, are bounded during this time interval so that the attitude rate of change is given by

$$\dot{R}_r(t) = R_r(t)\Omega_r(t)^{\times}, \quad \text{given} \quad R_r(0), \Omega_r(t). \tag{4.4}$$

The attitude and angular velocity tracking error is defined as

$$Q(t) := R_r^T(t)R(t), \quad \omega(t) := \Omega(t) - Q^T(t)\Omega_r(t). \tag{4.5}$$

Equations (4.4) and (4.5) lead to the attitude error kinematics equation

$$\dot{Q}(t) = Q(t)(\Omega(t) - Q^T(t)\Omega_r(t))^\times = Q(t)\omega^\times(t). \tag{4.6}$$

Note that the attitude error kinematics is also "left invariant" like the original attitude kinematics (3.1), i.e., if $Q_l = CQ$, where $C \in \mathrm{SO}(3)$ is constant, then $\dot{Q}_l = Q_l\omega^\times$.

Rewriting the attitude dynamic equation (4.3) in terms of the tracking errors, we obtain

$$\begin{aligned} J\dot{\omega} =& J(\omega^\times Q^T\Omega - Q^T\dot{\Omega}_r) - (\omega + Q^T\Omega_r)^\times J(\omega + Q^T\Omega_r) \\ &+ M_b(R_rQ) + \tau, \end{aligned} \tag{4.7}$$

where $M_b(R_rQ) = -r_{C_B} \times (\rho g\mathcal{V})(R_rQ)^T e_3$. Note, the trajectory tracking error kinematic and dynamic Eqs. (4.6) and (4.7), respectively, depend on $Q, \omega, \Omega_r, \dot{\Omega}_r$, and the control moment τ.

4.3 Control Law for Tracking the Reference Trajectory

In this section, we provide the control law that achieves the control task of asymptotically tracking the desired attitude and angular velocity given by (4.4), following the kinematics and dynamics (4.6) and (4.7). The controller obtained achieves almost global asymptotic tracking, i.e., the attitude and angular velocity converge to the desired trajectory from all initial conditions, except those that lie in a subset of zero volume in the state space.

Before we move ahead, we provide some Definitions and a Lemma that we will be making use of in this section. We discuss Morse Lemma and its immediate corollaries which will be important for our feedback control design. For the proofs of these results, we refer the reader to [44]. Let M be an m dimensional manifold without boundary and $f : M \to \mathbb{R}$ a smooth function defined on it.

Definition 4.2. (Critical points of f). A point $p_0 \in M$ is a critical point of M if we have

$$\frac{\partial f}{\partial x_1}(p_0) = 0, \frac{\partial f}{\partial x_2}(p_0) = 0, \ldots, \frac{\partial f}{\partial x_m}(p_0) = 0,$$

with respect to a local coordinate system $(x_1, x_2, \ldots, x_m)$ about p_0.

Definition 4.3. (Non-degenerate and degenerate critical points). We say that a critical point p_0 is *non-degenerate* if the determinant of the Hessian of f at p_0, $\det H_f(p_0)$ is not zero. We say that it is *degenerate* if $\det H_f(p_0) = 0$.

Definition 4.4. (Morse function). We say that a function $f : M \to \mathbb{R}$ is a Morse function

if every critical point of f is non-degenerate.

Lemma 4.1. *(Morse lemma for dimension m). Let p_0 be a non-degenerate critical point of $f : M \to \mathbb{R}$. Then we can choose a local coordinate system $(X_1, X_2, \ldots, X_m)$ about p_0 such that the coordinate representation of f with respect to these coordinates has the following standard form*

$$f = -X_1^2 - X_2^2 - \ldots - X_\lambda^2 + X_{\lambda+1}^2 + \ldots + X_m^2 + c,$$

where p_0 corresponds to the origin $(0, 0, \ldots, 0)$ and c is a constant ($= f(p_0)$).

Definition 4.5. (Index). The number λ is called the *index* of a non-degenerate critical point p_0. The index of p_0 lies in $[0, m)$.

Corollary 4.2. *A non-degenerate critical point is isolated.*

Corollary 4.3. *A Morse function defined on a compact manifold admits only finitely many critical points.*

Definition 4.6. (Class-$\mathcal{K}$ function). A function $\alpha(\cdot) : \mathbb{R}^+ \mapsto \mathbb{R}^+$ belongs to Class-$\mathcal{K}$ (denoted by $\alpha(\cdot) \in \mathcal{K}$) if it is continuous, strictly increasing and $\alpha(0) = 0$.

Let $\Phi : \mathbb{R}^+ \to \mathbb{R}^+$ be a $\mathcal{C}^2$ function that satisfies $\Phi(0) = 0$ and $\Phi'(x) > 0$ for all $x \in \mathbb{R}^+$. Let $\Phi'(\cdot) \leq \alpha(\cdot)$, where $\alpha(\cdot)$ is a Class-$\mathcal{K}$ function.

Next, let L and K be the positive definite control gain matrices, with $K = \text{diag}(k_1, k_2, k_3)$ such that $0 < k_1 < k_2 < k_3$. The control law design is based on a Lyapunov-type analysis on the state space $\text{TSO}(3)$ of the attitude dynamics.

Using Eq. (4.6), the time derivative of $\Phi(\text{trace}(K - KQ))$ (see [46]) is given by

$$\begin{aligned}\frac{d}{dt}\Phi(\text{trace}(K - KQ)) =& - \Phi'(\text{trace}(K - KQ))\text{trace}(KQ\omega^{\times}) \\ =& - \Phi'(\text{trace}(K - KQ))\omega^T[k_1 e_1^{\times} Q^T e_1 + k_2 e_2^{\times} Q^T e_2 + k_3 e_3^{\times} Q^T e_3].\end{aligned}$$

Based on the results of [46, 47], the following continuous control law to asymptotically track the desired attitude and angular velocity is proposed

$$\begin{aligned}\tau =& - L\omega + JQ^T\dot{\Omega}_r + (Q^T\Omega_r)^{\times} JQ^T\Omega_r \\ &+ \Phi'(\text{trace}(K - KQ))[k_1 e_1^{\times} Q^T e_1 + k_2 e_2^{\times} Q^T e_2 + k_3 e_3^{\times} Q^T e_3] - M_b(R_r Q),\end{aligned} \tag{4.8}$$

where $\Phi(\text{trace}(K - KQ))$ is a Morse function on $\mathrm{SO}(3)$ whose critical points are non-degenerate, and hence isolated according to the Morse Lemma. Note that this control law, and hence the trajectories of the closed-loop system, are smooth with respect to time and the error variables Q and ω.

In [46], the authors have shown that $(Q, \omega) = (\mathbb{I}, 0)$ is a stable equilibrium of the closed-loop system consisting of Eqs. (4.6), (4.7) and (4.8). Moreover, this equilibrium is almost global asymptotically stable, i.e., the domain of attraction is the whole state space (which is the tangent bundle $\mathrm{TSO}(3)$), except for a subset of volume measure zero.

Chapter 5
Asymptotic Feedback Tracking of an AUV in $\mathbf{SE(3)}$

Earlier, we have seen that the trajectory tracking in the state-space $\mathrm{TSE}(3)$ is a challenging problem with several applications to the control of underwater vehicles and spacecraft. In this chapter, we develop the theory for the asymptotic tracking of reference trajectories by an AUV in $\mathrm{TSE}(3),$ in the absence of disturbance inputs φ_ν^d and τ_Ω^d. From equation (3.2), the dynamic equations are given by

$$\begin{aligned} M\dot{\nu} &= M\nu \times \Omega + D_\nu(\nu)\nu + (W - \rho g\mathcal{V})R^T e_3 + \varphi_\nu, \\ J\dot{\Omega} &= J\Omega \times \Omega + M\nu \times \nu + D_\Omega(\Omega)\Omega - r_{C_B} \times (\rho g\mathcal{V})R^T e_3 + \tau_\Omega. \end{aligned} \tag{5.1}$$

5.1 Kinematics and Dynamics of Trajectory Tracking Error

The reference trajectory to be tracked by an AUV is given by the initial desired position vector in the inertial frame $b_r(0),$ the desired orientation $R_r(0)$ and the desired translational and angular velocity time profiles in the body frame, $\nu_r(t)$ and $\Omega_r(t),$ respectively. We discuss the design of reference trajectories in chapter 7.

The reference trajectory satisfies the following kinematic equation

$$\dot{g_r} = g_r\zeta_r, \tag{5.2}$$

where $g_r = \begin{bmatrix} R_r & b_r \\ 0 & 1 \end{bmatrix} \in \mathrm{SE}(3)$ and $\zeta_r = \begin{bmatrix} \Omega_r^{\times} & \nu_r \\ 0 & 0 \end{bmatrix} \in \mathfrak{se}(3)$.

We first define the trajectory tracking errors as follows:

$a(t) := b(t) - b_r(t) =$ error in inertial position,

$x(t) := R_r^T(t)a(t) =$ error in position expressed in reference body frame,

$Q(t) := R_r^T(t)R(t) =$ error in body attitude (orientation),

$\upsilon(t) := \nu(t) - Q^T(t)(\nu_r(t) + \Omega_r(t)^{\times}x(t)) =$ error in body translational velocity,

$\omega(t) := \Omega(t) - Q^T\Omega_r(t) =$ error in body angular velocity.

The above definitions and Eq. (5.2) lead us to the following kinematics for the error variables

$$\begin{aligned} \dot{x} &= Q\upsilon, \\ \dot{Q} &= Q\omega^{\times}. \end{aligned} \tag{5.3}$$

Equation (5.3) can be written in a compact form as $\dot{h} = h\xi$, where

$$h = \begin{bmatrix} Q & x \\ 0 & 1 \end{bmatrix} \in \mathrm{SE}(3),$$

and

$$\xi = \begin{bmatrix} \omega^{\times} & \upsilon \\ 0 & 0 \end{bmatrix} \in \mathfrak{se}(3).$$

Note that the kinematics of the error variables are in the standard left-invariant form on $\mathrm{SE}(3)$.

Let us define $\widetilde{\nu_r} := \nu_r + \Omega_r^{\times} x$. Now, we rewrite Eq. (5.1) by substituting $\omega + Q^T\Omega_r$ and $\upsilon + Q^T\nu_r$ for Ω and ν, respectively. Therefore we obtain the trajectory tracking dynamics given by

$$\begin{aligned} M\dot{\upsilon} =& M\{\omega^{\times}Q^T\widetilde{\nu_r} - Q^T\dot{\widetilde{\nu_r}}\} + M(\upsilon + Q^T\widetilde{\nu_r})^{\times}(\omega + Q^T\Omega_r) + D_{\nu}(\nu)(\upsilon + Q^T\widetilde{\nu_r}) \\ &+ (W - \rho g\mathcal{V})Q^T R_r^T e_3 + \varphi_{\nu}, \end{aligned} \tag{5.4}$$

$$\begin{aligned} J\dot{\omega} =& J(\omega^{\times}Q^T\Omega_r - Q^T\dot{\Omega}_r) - (\omega + Q^T\Omega_r)^{\times}J(\omega + Q^T\Omega_r) - (\upsilon + Q^T\widetilde{\nu_r})^{\times}M(\upsilon + Q^T\widetilde{\nu_r}) \\ &+ D_{\Omega}(\Omega)(\omega + Q^T\Omega_r) - r_{CB} \times (\rho g\mathcal{V})Q^T R_r^T e_3 + \tau_{\Omega}. \end{aligned} \tag{5.5}$$

So, the trajectory tracking error kinematics and dynamics are given by Eqs. (5.3), (5.4) and (5.5).

We will see in the next section that the control law for feedback tracking depends on $x,$ error in position in the reference body frame. However, if we exclude the control forces and moments, then the Eqs. (5.4) and (5.5), involving the dynamics of the tracking error, are independent of the tracking error in position, which is given by a or x.

Next we give the control law that achieves the control task of tracking the desired position and velocity as specified by the reference trajectory while following the kinematic and dynamic equations given by Eqs. (5.3)-(5.5). The control law design in based on a Lyapunov-type analysis on the nonlinear state-space $\mathrm{TSE}(3)$ of the AUV dynamics.

5.2 Control Law for Almost Global Asymptotic Tracking

Here, we provide a control law that achieves the control task of almost global asymptotically tracking the reference trajectory in $\mathrm{SE}(3)$. The almost global asymptotic tracking performance ensures that the actual trajectory of the AUV converges to the reference trajectory asymptotically for almost all initial tracking errors except for a set of measure zero in the state space, $\mathrm{TSE}(3)$.

In Section 4.3, we developed a control law for asymptotically tracking the desired attitude and angular velocity. Here, we use the Definitions and results from Section 4.3 to give the control law for trajectory tracking in $\mathrm{SE}(3)$. The feedback tracking control scheme is based on Lyapunov-type analysis. We assume that we have the measurements or can estimate all the "tracking error" states, i.e., x, v, Q and ω.

Let $\Phi : \mathbb{R}^+ \to \mathbb{R}^+$ be a $\mathcal{C}^2$ function that satisfies $\Phi(0) = 0$ and $\Phi'(u) > 0$ for all $u \in \mathbb{R}^+$. Let $\Phi'(\cdot) \leq \alpha(\cdot)$, where $\alpha(\cdot)$ belongs to class-$\mathcal{K}$ function (denoted by $\alpha(\cdot) \in \mathcal{K}$). Also, let K, L_ν, L_Ω and N be positive definite control gain matrices, with $K = \mathrm{diag}(k_1, k_2, k_3)$ such that $0 < k_1 < k_2 < k_3$. Therefore $\Phi(\mathrm{trace}(K - KQ))$ is a Morse function on $\mathrm{SO}(3)$, where $Q \in \mathrm{SO}(3)$. The critical points of $\Phi(\mathrm{trace}(K - KQ))$ are non-degenerate, and hence isolated according to the Morse Lemma (see Section 4.3).

Along the kinematics, given by Eq. (5.3), the time derivative of $\Phi(\text{trace}(K - KQ))$ (see [46]) is given by

$$\begin{aligned}\frac{d}{dt}\Phi(\text{trace}(K - KQ)) =& - \Phi'(\text{trace}(K - KQ))\text{trace}(KQ\omega^{\times}) \\ =& - \Phi'(\text{trace}(K - KQ))\omega^{T}[k_1 e_1^{\times} Q^T e_1 + k_2 e_2^{\times} Q^T e_2 + k_3 e_3^{\times} Q^T e_3].\end{aligned} \tag{5.6}$$

We propose the following control laws for φ_ν and τ_Ω to asymptotically track the reference trajectory in $\mathrm{TSE}(3)$

$$\begin{aligned}\varphi_\nu =& - L_\nu \upsilon + MQ^T\dot{\widetilde{\nu}}_r + (Q^T\Omega_r)^{\times}(M(\upsilon + Q^T\widetilde{\nu}_r)) - D_\nu(\nu)(\upsilon + Q^T\widetilde{\nu}_r) \\ & - (W - \rho g\mathcal{V})Q^T R_r^T e_3 - Q^T N x,\end{aligned} \tag{5.7}$$

$$\begin{aligned}\tau_\Omega =& -L_\Omega\omega + JQ^T\dot{\Omega}_r + (Q^T\Omega_r)^{\times}(JQ^T\Omega_r) + (Q^T\widetilde{\nu}_r)^{\times}(MQ^T\widetilde{\nu}_r) \\ & - D_\Omega(\Omega)(\omega + Q^T\Omega_r) + (\rho g\mathcal{V})r_{CB}^{\times}(Q^T R_r^T e_3) \\ & + \Phi'(\text{trace}(K - KQ))[k_1 e_1^{\times} Q^T e_1 + k_2 e_2^{\times} Q^T e_2 + k_3 e_3^{\times} Q^T e_3].\end{aligned} \tag{5.8}$$

It is to be noted that the control law, and hence the trajectories of the closed-loop system, are continuous with respect to the error variables x, υ, Q and ω.

Chapter 6
Lyapunov Analysis of the Feedback Tracking Control Scheme

In [46, 47], the authors have shown that a control law, similar to the one proposed in Chapter 4, asymptotically tracks the desired attitude and angular velocity trajectory of a spacecraft. The attitude dynamics of an AUV was modeled in Chapter 4 with the assumption that there is a disturbance moment, and that the translational velocity is zero. Under these assumptions, the attitude dynamics of an AUV are similar to that of a spacecraft. So, the asymptotic properties of the trajectory tracking errors in $\mathrm{TSO}(3)$ follows from the analysis done in [46, 47].

Before we proceed, we discuss some important concepts which will be of use in this section.

Asymptotic stability of a control system is an important property to be determined. Lyapunov's stability theorems studied in Chapter 4 are often difficult to apply to establish this property, as it often happens that the derivative of the Lyapunov function candidate $\dot{\psi}$ is only negative semi-definite. In this situation, it is still possible to draw conclusions on asymptotic stability with the help of the *invariant set* theorem, which is attributed to LaSalle.

Definition 6.1. (Invariant Set). Let X be a smooth vector field on a manifold M.

1. A set $A \subset M$ is X-invariant (or invariant for X) if, for all $x \in A$, the integral curve $\mathbb{R} \ni t \mapsto \Phi_t^X(x)$ takes values in A.

2. A set $A \subset M$ is positively X-invariant if, for all $x \in A$, the integral curve $\overline{\mathbb{R}}^+ \ni t \mapsto \Phi_t^X(x)$ takes values in A, where $\overline{R}^+ = \{x \in \mathbb{R} | x \geq 0\}$.

Now we state the important LaSalle's Invariance Principle, the proof of which can be found in [7].

Theorem 6.1. *(LaSalle Invariance Principle). For $X \in \Gamma^\infty(M)$, let $A \subset M$ be compact and positively X-invariant. Let the Lie-derivative of $\psi \in \mathcal{C}^\infty(M)$, with respect to X, satisfy $\mathscr{L}_X\psi(x) \leq 0$ for all $x \in A$, and let B be the largest positively X-invariant set contained in $\{x \in A | \mathscr{L}_X\psi(x) = 0\}$. Then the following statements hold:*

1. *each integral curve of X with initial condition in A approaches B as $t \to +\infty$;*

2. *if B consists of a finite number of isolated points, then each integral curve of X with initial condition in A converges to a point of B as $t \to +\infty$.*

Thus, LaSalle's principle is a useful extension of Lyapunov Stability theory.

Definition 6.2. (Domain of Attraction). The domain of attraction of an equilibrium point x_0, is the largest set $D(X, x_0)$ such that, for all $x \in D(X, x_0), \Phi_t^X(x)$ converges to x_0 as $t \to +\infty, i.e., \quad D(X, x_0) = \{x \in M | \lim_{t \to +\infty} \Phi_t^X(x) = x_0\}$.

Remark 6.1. The domain of attraction of an equilibrium point x_0 is also an invariant set.

Now, we are ready to show the asymptotic properties of the trajectory tracking errors in $\mathrm{TSE}(3)$ by analyzing the closed-loop system presented in Chapter 5.

6.1 Critical Points for the Closed-Loop Attitude Dynamics

In this section, we present a Lemma from [46]. We will be using this to prove the main result on asymptotic trajectory tracking.

Lemma 6.1. *The function* $\Phi(\mathit{trace}(K - KQ))$ *on* $\mathrm{SO}(3)$ *has the set of non-degenerate critical points*

$$E_c = \{\mathbb{I}, \mathit{diag}(-1, 1, -1), \mathit{diag}(1, -1, -1), \mathit{diag}(-1, -1, 1)\} \tag{6.1}$$

Further, the unique minimum point of this function is $Q = \mathbb{I} = \mathit{diag}(1, 1, 1)$.

Proof. As discussed earlier, the function $\Phi(\mathrm{trace}(K - KQ))$ on $\mathrm{SO}(3)$ is a Morse function, and has a set of non-degenerate critical points. The gain matrix, $K = \mathrm{diag}(k_1, k_2, k_3)$, with $0 < k_1 < k_2 < k_3$, is a positive definite diagonal matrix. Let $\langle \cdot \rangle$ denote the trace inner product on the vector space $\mathbb{R}^{n \times n}$ given by $\langle A, B \rangle = \mathrm{trace}(A^T B)$. The critical points of Φ

are given by equating its first variation to zero

$$\begin{aligned}\partial\Phi(\text{trace}(K-KQ)) &= \Phi'(\text{trace}(K-KQ))\partial\text{trace}(K-KQ)\\ &= \Phi'(\text{trace}(K-KQ))\partial\langle K, I-Q\rangle\\ &= -\Phi'(\text{trace}(K-KQ))\langle K, \partial Q\rangle = 0.\end{aligned}$$

Let the variation on $\mathrm{SO}(3)$ be given by $\partial Q = QU$, where $U \in \mathfrak{so}(3)$. Since $\Phi'(x) > 0$ for $x > 0$, we get the criticality condition

$$\langle K, \partial Q\rangle = \langle K, QU\rangle = 0,$$

which is equivalent to KQ being symmetric (since U is skew-symmetric). Let $KQ = S = S^T$, which implies that $Q = K^{-1}S$.

As $Q \in \mathrm{SO}(3)$, we have $QQ^T = \mathbb{I} \Leftrightarrow K^{-1}S^2K^{-1} = \mathbb{I} \Leftrightarrow S^2 = K^2$. Also since $\det Q = 1$, the set of solutions $\mathcal{S}$ of S for the above equation is given by

$$\mathcal{S} = \{K, \text{diag}(-k_1, k_2, -k_3), \text{diag}(k_1, -k_2, -k_3), \text{diag}(-k_1, -k_2, k_3)\}.$$

This leads to the set of four critical points given by Eq. (6.1).

To find the minimum of the function $\Phi(\text{trace}(K - KQ))$ in $\mathrm{SO}(3)$, we set its second vari-

ation, with respect to Q at a critical point, to be positive

$$\begin{aligned}\partial^2\Phi(\text{trace}(K - KQ)) = -\Phi'(\text{trace}(K - KQ))\langle K, QU^2\rangle > 0,\\ \Leftrightarrow -\langle K, QU^2\rangle > 0,\\ \Leftrightarrow \text{trace}(KQU^2) > 0.\end{aligned}$$

Note that we have assumed $\Phi'' = 0$. Now, since $U^2 \geq 0$ for $U \in \mathfrak{so}(3)$, the above condition is equivalent to $KQ = S$ being positive definite. From the set of critical points $\mathcal{S}$ for S, we see that the only positive definite solution is $S_0 = K = \text{diag}(k_1, k_2, k_3)$. So, we get a unique minimum point of $\Phi(\text{trace}(K - KQ))$ in $\text{SO}(3)$ as $Q = S_0^{-1}K = \mathbb{I}$. □

Using this result, we will show almost global asymptotic stability of the equilibrium $(x_e, Q_e, v_e, \omega_e) = (0, \mathbb{I}, 0, 0) \in \text{TSO}(3) \times \mathbb{R}^6 \simeq \text{TSE}(3)$ in the next section.

6.2 Asymptotic Convergence Results

For the closed-loop dynamics of the AUV, we first prove the local asymptotic stability of the equilibrium $(\mathbb{I}, 0) \in \text{TSO}(3)$, when $(v, \omega) = (0, 0)$. Before discussing our main Theorem, we give the following Lemma, the proof of which can be found in [46].

Lemma 6.2. *The equilibrium* $(\mathbb{I}, 0)$ *of the closed-loop attitude dynamics given by Eq.* (5.5) *and the control law given in Eq.* (5.8) *is locally asymptotically stable when* $(v, \omega) = (0, 0)$. *The other equilibria given by* $(Q_e, 0)$*, where* $Q_e \in E_c \setminus \{\mathbb{I}\}$*, of the closed-loop attitude*

dynamics under these conditions are unstable. Furthermore, under these conditions the set of all initial conditions converging to the equilibrium $(Q_e, 0)$*, where* $Q_e \in E_C \setminus \{\mathbb{I}\}$ *form a lower dimensional manifold.*

The next theorem gives the main result regarding the asymptotic convergence of the tracking error dynamics for the closed-loop dynamics in Eqs. (5.4)-(5.8) to the desired equilibrium $(x_e, Q_e, \upsilon_e, \omega_e) = (0, \mathbb{I}, 0, 0)$.

Theorem 6.2. *The trajectories of the closed-loop tracking error system given by the dynamics in Eqs.* (5.4)-(5.8) *converge to the set*

$$\mathcal{E} = \{(x, Q, \upsilon, \omega) \in \mathrm{TSE}(3) : \upsilon = 0, \omega = 0, x = 0, Q \in E_c\}, \tag{6.2}$$

where E_c *is as defined in Eq.* (6.1)*. Further, the equilibrium* $(x_e, Q_e, \upsilon_e, \omega_e) = (0, \mathbb{I}, 0, 0)$ *of the closed-loop system is asymptotically stable in this case and its domain of attraction is almost global.*

Proof. For the closed-loop tracking error dynamics given by Eqs. (5.4)-(5.8), we propose the following candidate Lyapunov function

$$V(x, Q, \upsilon, \omega) = V_T(x, \upsilon) + V_A(Q, \omega), \tag{6.3}$$

where $V_T(x, \upsilon) = \frac{1}{2}\upsilon^T M \upsilon + \frac{1}{2} x^T N x$, and $V_A(Q, \omega) = \frac{1}{2}\omega^T J \omega + \Phi(\mathrm{trace}(K - KQ))$. Note that $V(x, Q, \upsilon, \omega) \geq 0$ and its "attitude component" $V_A(Q, \omega) = 0$ if and only if $(Q, \omega) = (\mathbb{I}, 0)$. Thus, $V(x, Q, \upsilon, \omega)$ is a positive-definite function on $\mathrm{TSE}(3)$ which is

zero only at the desired equilibrium.

We now obtain the time derivative of this Lyapunov function, using the time derivative of $\Phi(\text{trace}(K - KQ))$ along the trajectories of the closed-loop system, which we obtained in Eq. (5.6). We evaluate the time derivative of $V(x, Q, \upsilon, \omega)$ along the trajectories of the closed-loop system given by Eqs. (5.4)-(5.5) and the control laws in Eqs. (5.7)-(5.8). The time derivative of $V_T(x, \upsilon)$ along (5.4) and (5.7) is

$$\begin{aligned}
\dot{V}_T &= \upsilon^T M\dot{\upsilon} + x^T N\dot{x} \\
&= \upsilon^T[M(\omega^\times Q^T\widetilde{\nu}_r) - MQ^T\dot{\widetilde{\nu}}_r] + (M(\upsilon + Q^T\widetilde{\nu}_r))^\times(\omega + Q^T\Omega_r) + D_\nu(\nu)(\upsilon + Q^T\widetilde{\nu}_r) \\
&\quad + (W - \rho g\mathcal{V})Q^T R_r^T e_3 + Q^T Nx + \varphi_\nu(x, Q, \upsilon)] \\
&= \upsilon^T[M(\omega^\times Q^T\widetilde{\nu}_r) + (M(\upsilon + Q^T\widetilde{\nu}_r))^\times\omega - L_\nu\upsilon].
\end{aligned} \tag{6.4}$$

The time derivative of $V_A(Q, \omega)$ along Eqs. (5.5), (5.6) and (5.8) is

$$\begin{aligned}
\dot{V}_A &= \omega^T J\dot{\omega} - \Phi'(\text{trace}(K - KQ))\omega^T[k_1 e_1^\times Q^T e_1 + k_2 e_2^\times Q^T e_2 + k_3 e_3^\times Q^T e_3] \\
&= \omega^T\Big[J(\omega^\times Q^T\Omega_r - Q^T\dot{\Omega}_r) - (Q^T\Omega_r)^\times J(\omega + Q^T\Omega_r) - (\upsilon + Q^T\widetilde{\nu}_r)^\times M(\upsilon + Q^T\widetilde{\nu}_r) \\
&\quad - r_{CB}^\times(\rho g\mathcal{V})Q^T R_r^T e_3 + D_\Omega(\Omega)(\omega + Q^T\Omega_r) \\
&\quad - \Phi'(\text{trace}(K - KQ))[k_1 e_1^\times Q^T e_1 + k_2 e_2^\times Q^T e_2 + k_3 e_3^\times Q^T e_3] + \tau_\Omega(Q, \upsilon, \omega)\Big] \\
&= \omega^T[J(\omega^\times Q^T\Omega_r) - (Q^T\Omega_r)^\times J\omega - \upsilon^\times M(\upsilon + Q^T\widetilde{\nu}_r) - (Q^T\widetilde{\nu}_r)^\times M\upsilon - L_\Omega\omega] \\
&= -\omega^T[\upsilon^\times M(\upsilon + Q^T\widetilde{\nu}_r) + (Q^T\widetilde{\nu}_r)^\times M\upsilon + L_\Omega\omega].
\end{aligned} \tag{6.5}$$

Therefore combining Eqs. (6.4) and (6.5) and using the scalar triple product identity, we get

$$\dot{V} = \dot{V}_T + \dot{V}_A = -\upsilon^T L_\nu \upsilon - \omega^T L_\Omega \omega \leq 0,$$

and $\dot{V} = 0$ iff $\upsilon = 0$ and $\omega = 0$.

Recall that $\Phi(\cdot)$ is a strictly increasing monotone function. Thus, for any $(x(0), Q(0), \upsilon(0), \omega(0)) \in \mathrm{TSE}(3)$, the set

$$\mathcal{I} = \{(x, Q, \upsilon, \omega) \in \mathrm{TSE}(3) : V(x, Q, \upsilon, \omega) \leq V(x(0), Q(0), \upsilon(0), \omega(0))\},$$

is an invariant set of the closed-loop system [9, 46]. Now, by LaSalle's invariant set Theorem, it follows that all solutions that begin in $\mathcal{I}$ converge to the largest invariant subset of $\dot{V}^{-1}(0)$ contained in $\mathcal{I}$. Since $\dot{V}(x, Q, \upsilon, \omega) \equiv 0$ implies $\upsilon = \omega \equiv 0$, we substitute this into the closed-loop system equations to get

$$\begin{aligned}
\dot{V}^{-1}(0) =& \{(x, Q, \upsilon, \omega) \in \mathrm{TSE}(3) : \upsilon \equiv 0, \omega \equiv 0, Q^T N x \equiv 0, \\
& \Phi'(\text{trace}(K - KQ))\text{trace}(KQ\omega^\times) \equiv 0\} \\
\Rightarrow \dot{V}^{-1}(0) =& \{(x, Q, \upsilon, \omega) \in \mathrm{TSE}(3) : \upsilon \equiv 0, \omega \equiv 0, \\
& x \equiv 0, k_1 e_1^\times Q^T e_1 + k_2 e_2^\times Q^T e_2 + k_3 e_3^\times Q^T e_3 \equiv 0\} \\
=& \{(x, Q, \upsilon, \omega) \in \mathrm{TSE}(3) : x \equiv 0, Q \in E_c, \upsilon \equiv 0, \omega \equiv 0\},
\end{aligned}$$

since $Q^T N x = 0 \Rightarrow x = 0$ as $Q \in \mathrm{SO}(3)$ is invertible and N is positive definite. In this case, each of the four points given by Eq. (6.2) are an equilibrium of the closed-loop dynamics in $\mathrm{TSE}(3)$. Therefore, by LaSalle's Theorem, all solutions of the closed-loop system converge to one of the equilibria in $\mathcal{E} \cap \mathcal{I}$, where $\mathcal{E}$ is given by Eq. (6.2).

From Lemma 6.2, we see that the only stable equilibrium in this equilibrium set is $(x, Q, v, \omega) = (0, \mathbb{I}, 0, 0)$. In fact, as stated in Lemma 6.2, all solutions that converge to the other three equilibria form a lower dimensional manifold. Thus, this set of solutions has measure zero in $\mathrm{TSE}(3)$ (see also [9, 46]). Solutions of the closed-loop system that do not start in this manifold, thus converge asymptotically to the stable equilibrium $(x, Q, v, \omega) = (0, \mathbb{I}, 0, 0)$. Therefore, the domain of attraction of this equilibria is almost global. □

Remark 6.2. Since this is also the desired equilibrium for asymptotic tracking, the closed-loop system performs almost global asymptotic tracking in this case.

Chapter 7
Design of Reference Trajectory

In the previous two chapters, we have formulated the feedback control dynamics for the two problems at hand: the attitude tracking problem in $\mathrm{SO}(3)$, and the trajectory tracking problem in $\mathrm{SE}(3)$. We have seen that the feedback dynamics depend on the reference trajectory to be tracked. In this chapter, we discuss the methods employed for designing the reference trajectory.

For the attitude trajectory tracking in $\mathrm{SO}(3)$, the reference trajectory is given by the initial attitude $R_r(0)$ and the angular velocity as a function of time $\Omega_r(t)$, for some interval of time $t \in [0, T]$, where $T > 0$. Also $\|\Omega_r(t)\| \leq C_1$ and $\|\dot{\Omega}_r(t)\| \leq C_2$ for $0 < t \leq T$, where $C_i (i = 1, 2)$ is a constant. We will give the explicit equations for the attitude time trajectory and the desired angular velocity time profile in the next Chapter, where we deal with simulation of the feedback dynamics.

7.1 Reference Trajectory in $\mathrm{TSE}(3)$

The design of a reference trajectory for $\mathrm{TSE}(3)$ merits a detailed discussion. The reference trajectory has been taken from different mission scenarios which have already been implemented on the test-bed AUV, ODIN, and which have been presented in [50]. It is relevant, as well as interesting, to know how these missions were implemented on ODIN using geometric control techniques. However, we should note that the motion planning

problem using geometric control techniques is in itself a separate research topic and out of the scope of this thesis. A detailed description of the design of open-loop control strategies for the motion of a test-bed AUV can be found in [50].

Since the scope of this thesis is not to study the methods employed for generating the control forces, we do a brief review of the control design process using a *kinematic reduction and decoupling vector fields*, as is detailed in [50]. A detailed discussion of these concepts can also be found in [7].

We are interested in the open-loop control forces and moments that have been derived in [50] for different mission scenarios. We use these controls to numerically solve the system of equations given in Lemma 3.1; this gives us the reference trajectory.

7.1.1 Kinematic Reduction and Decoupling Vector Fields

Let Q be the configuration space of the system. From [50], we have the following Lemma

Lemma 7.1. *Let $Q = \mathrm{SE}(3), \widetilde{\nabla}$ be the modified Levi-Civita connection on the configuration space Q associated with the Riemannian metric $\mathbb{G}$ and let the set of input control vector fields be given by $\mathcal{I} = \{\mathbb{I}^{-1}, \ldots, \mathbb{I}^{-1}\}$. Let $G^{\#}P(\gamma(t))$ represent the restoring forces arising from gravity and buoyancy. Then, the equations of motion of a rigid body submerged in a viscous fluid are given by the forced affine connection control system:*

$$\widetilde{\nabla}_{\gamma'}\gamma' = G^{\#}P(\gamma(t)) + \sum_{i=1}^{6} \mathbb{I}^{-1}(\gamma(t))\sigma_i(t), \tag{7.1}$$

where $\sigma_i(t)$ represent the controls.

Note that the viscous drag forces have been included in the modified Levi-Civita connection. The restoring forces and moments due to gravity and buoyancy can not be included in this connection as these forces depend on the orientation of the body and not on its velocity or acceleration. Also note that Eq. (7.1) is a second-order system on Q.

The motion planning problem for a second-order system on Q can be reduced to a first-order system on Q by use of a kinematic reduction, with the property that the controlled trajectory (i.e. solutions) of the reduced system are also the controlled trajectories of the original second-order system, with the exception of a possible "reparameterization". This method of reducing the complexity of the system to solve dynamic control problems has been previously reported in [6, 8]. In [7], the authors have explained this topic in great detail.

We denote an affine connection control system (dynamic) by $\Sigma_{dyn} = (Q, \nabla, \mathcal{Y}, \mathbb{R}^6)$. The associated driftless system (kinematic) is the triple $\Sigma_{kin} = (Q, \mathcal{X} = \{X_1, \ldots, X_{\widetilde{m}}\}, U)$, where $\mathcal{X} \in \Gamma^\infty(TQ), U \subset \mathbb{R}^{\widetilde{m}}, \widetilde{m} \leq 6$. Here $\Gamma^\infty(TQ)$ represents the $\mathcal{C}^\infty$-section of the distribution generated by TQ, the tangent bundle of Q. The driftless system is associated to the affine control system defined by

$$\gamma'(t) = \sum_{\alpha=1}^{\widetilde{m}} \widetilde{u}^\alpha(t) X_\alpha(\gamma(t)), \tag{7.2}$$

where a controlled trajectory is a pair $(\gamma, \widetilde{u})$ such that

1. $\gamma : I \to Q$ and $\widetilde{u} : I \to U$ are both defined on the same interval $I \subset \mathbb{R}$,

2. $\widetilde{u}$ belongs to the class of kinematic inputs $\mathcal{U}_{kin}^{\widetilde{m}}$,

3. $(\gamma, \widetilde{m})$ together satisfy Eq. (7.2).

Definition 7.1. (Kinematic Reduction). Let $\Sigma_{dyn} = (Q, \nabla, \mathcal{Y}, \mathbb{R}^m)$ be a $\mathcal{C}^\infty$ affine connection control system with $\mathscr{Y}$ having locally constant rank. A driftless system $\Sigma_{kin} = (Q, \mathcal{X}, \mathbb{R}^{\widetilde{m}}), (\widetilde{m} \leq 6)$ is a kinematic reduction of Σ_{dyn} if

1. $\mathscr{X}$ is a locally constant rank subbundle of TQ, and if

2. for every controlled trajectory (γ, u_{kin}) for Σ_{kin} with $u_{kin} \in \mathcal{U}_{kin}^{\widetilde{m}}$, there exists $u_{dyn} \in \mathcal{U}_{dyn}^{m}$ such that (γ, u_{dyn}) is a controlled trajectory of Σ_{dyn}.

Here, $\mathcal{Y}$ are the input vector fields for an affine connection control system, and $\mathscr{Y}$ is a distribution generated by them. The distribution generated by the input control vector fields for the kinematic system $\mathcal{X}$ are given by $\mathscr{X}$.

The rank of a kinematic reduction Σ_{kin} at $q \in Q$ is the rank of $\mathscr{X}$ at q. In particular, a rank-one kinematic reduction is called *decoupling vector field*. The design of control strategies for the motion planning problems presented in [50] has been done by use of decoupling vector fields.

7.1.2 Open-Loop Control Design

Given an initial and a final configuration, η_i and η_f, respectively, the motion planning problem can be solved by determining a sequence of integral curves of decoupling vector fields to follow connecting η_i to η_f. We then parameterize each segment to start and end at zero velocity so that each segment begins with the same initial and final conditions and that the segments can be concatenated to build the entire trajectory. The dynamic, open-loop controls that steer the vehicle from η_i to η_f can be constructed from this reparameterized, concatenated, kinematic motion trajectory (see [50] for details).

It should be noted that by use of this method, we get a control strategy for a drift-free affine connection control system. However, as already mentioned in Lemma 7.1, the affine connection control system of an AUV is not driftless. In [50], the author has suggested a method of dealing with drift vector fields so that the calculated control scheme can be implemented onto a test-bed AUV.

We have briefly outlined a method for designing open-loop, dynamic controls which can be implemented on a test-bed AUV. In our present work, we will use the control forces that have been designed in [50]. We use these control forces while solving the ordinary differential equations given in lemma 3.1. We solve this system of equations using a fourth-order Runge-Kutta (RK) method to find the translational and angular velocities as well as translational and angular accelerations. Thus we get the reference trajectory.

Chapter 8
Numerical Schemes Used for Simulations

In this chapter, we discuss the various numerical schemes that have been used to simulate the feedback dynamics discussed in Chapters 4 and 5. The various numerical schemes that have been employed in this thesis are

1. *Feedback Trajectory Tracking in* $\mathrm{SO}(3)$*.*We use a Lie group variational integrator to simulate the feedback attitude dynamics discussed in Chapter 4. We also use a fourth-order RK coupled with a CG numerical scheme to simulate the attitude feedback dynamics. We will compare the results obtained by both of these methods in Chapter 9.

2. *Feedback Trajectory Tracking in* $\mathrm{SE}(3)$.We use a fourth-order RK coupled with a CG numerical scheme to simulate the feedback dynamics of an AUV discussed in Chapter 5.

We first present a discussion on differential equations on Lie groups and the application of CG method to solve the equations. Next, in Section 8.2, we obtain a discrete model of the continuous feedback attitude dynamics model presented in Chapter 4.

8.1 Differential Equations on Lie Groups

In this section, we study differential equations on a matrix Lie group.

Definition 8.1. (Lie Group). A Lie group is a group G that is also a differentiable manifold such that, for any $a, b \in G$, the multiplication $(a, b) \mapsto ab$ and inverse $a \mapsto a^{-1}$ are smooth maps.

Definition 8.2. (Lie Algebra).A Lie Algebra V is a $\mathbb{R}$-vector space endowed with a bilinear operation $[\cdot, \cdot] : V \times V \to V$ called the *bracket* satisfying

1. anti-commutativity, i.e., $[\xi, \eta] = -[\eta, \xi], \quad \forall \xi, \eta \in V$, and

2. the Jacobi identity, i.e., $[\xi, [\eta, \zeta]] + [\eta, [\zeta, \xi]] + [\zeta, [\xi, \eta]] = 0, \quad \forall \xi, \eta, \zeta \in V.$

A matrix Lie group is an example of a Lie group, whereas a matrix Lie algebra is an example of a Lie algebra.

A differential equation on a matrix Lie group, denoted by G, is an equation of the form

$$\dot{Y} = A(Y)Y, \quad Y(0) = Y_0 \in G, \tag{8.1}$$

where $A(Y) \in \mathfrak{g}$ and $Y \in G$ with $\mathfrak{g}$ denoting the Lie algebra of G (see [23]). As the tangent space at $Y \in G$ has the form $T_Y G = \{AY | A \in G\}$, the solution of Eq. (8.1) satisfies $Y(t) \in G$.

One has to be very cautious in numerically integrating the differential Eq. (8.1). The numerical method may have the shortcoming that, even when $Y_n \in G$, the update Y_{n+1} may not belong to the Lie group any more. In particular, solving Eq. (8.1) by Runge-Kutta method may lead to the iterates of Y drifting away from the manifold. Equation (8.1) can be solved using CG method or by Munthe-Kass method (see [23]). In our case, we will be using the former.

8.1.1 Crouch-Grossman Method

In CG method, the update is done by the exponential map, $\exp(ahA(Y_n))Y_n$. The method is described below (see [23]).

For $i = 1, 2, \ldots, s$

$$Y^{(i)} = \exp(ha_{i,i-1}K_{i-1}).\ldots.\exp(ha_{i,1}K_1)Y_n,$$

$$K_i = A(Y^{(i)}),$$

$$Y_{n+1} = \exp(hb_sK_s).\ldots.\exp(hb_1K_1),$$

where $a_{i,j}$ and b_j are integration parameters describing the particular explicit method. For $G = \mathrm{SO}(3)$, the exponential map $\exp(\omega^\times), \omega^\times \in \mathfrak{so}(3)$ is given by $e^{\omega^\times} = \mathbb{I} + \omega^\times + \frac{\omega^{\times 2}}{2!} +$

$\frac{\omega^{\times 3}}{3!} + \ldots$, which can be written in closed form solution as

$$e^{\omega^{\times}} = \mathbb{I} + \frac{\omega^{\times}}{\|\omega\|}\sin\|\omega\| + \frac{\omega^{\times 2}}{\|\omega\|^2}(1 - \cos\|\omega\|).$$

This is known as *Rodrigue's formula*.

Equation (8.1) asserts that $ahA(Y_n)$ does indeed belong to the associated Lie algebra. By the property of the exponential map, and by the construction of the update operation, the method of CG gives rise to approximation Y_{n+1} which lies exactly on the manifold defined by the Lie group. The accuracy of CG method is indicated by the order condition [23], which is determined by the coefficient a_{ij}, b_i and c_j for $i, j = 1, 2, \ldots, s$. The variable s denotes the stage of the algorithm.

8.2 Variational Integration of the Feedback Attitude Dynamics

The idea behind variational integrators is to discretize the variational principles of mechanics: *Hamilton's principle* for a conservative system or the *Lagrange-d'Alembert principle* for a system with non-conservative forcing [42]. In [34], a variational integrator was obtained by discretizing *Hamilton's principle*.

Here, we obtain a Lie group variational integrator by discretizing the *Lagrange-d'Alembert principle*. Next, we present a discrete Lagrange-d'Alembert principle for the continuous feedback attitude dynamics of an AUV discussed in Chapter 4.

8.2.1 Discrete Lagrange-d'Alembert Principle

The Lagrangian of the rigid body attitude dynamics discussed in Section 4.2 can be expressed as

$$\mathcal{L}(R,\Omega) = \frac{1}{2}\langle \Omega^{\times}, \mathcal{J}\Omega^{\times}\rangle - U(R), \tag{8.2}$$

where $\langle\cdot,\cdot\rangle$ is the trace inner product on $\mathbb{R}^{3\times 3}$ given by $\langle A, B\rangle = \text{trace}[A^T B]$, for all $A, B \in \mathbb{R}^{3\times 3}$. The moment of inertia matrix $\mathcal{J}$ can be expressed in terms of the standard moment of inertia matrix by $\mathcal{J} = \text{trace}[J]\mathbb{I} - J$, where $\mathbb{I}$ is the 3×3 identity matrix. The angular momentum $\Pi = J\Omega$ can be expressed in terms of $\mathcal{J}$ as follows

$$\Pi^{\times} = (J\Omega)^{\times} = \Omega^{\times}\mathcal{J} + \mathcal{J}\Omega^{\times}. \tag{8.3}$$

The continuous Lagrange-d'Alembert principle for the system given in Eqs. (4.3) and (4.8) can be given as

$$\delta \int_0^T \mathcal{L}(R(t),\Omega(t))dt + \int_0^T \langle \tau^{\times}(R,\Omega), \Sigma^{\times}\rangle = 0, \tag{8.4}$$

where Σ and $\delta\Omega$ are the permissible variations of R and Ω on $\mathrm{TSO}(3)$, respectively. These

possible variations, also known as *reduced variations* [43], can be expressed as

$$\delta R = R\Sigma^{\times}, \quad \delta\Omega = \dot{\Sigma} + \Omega \times \Sigma.$$

Let $h = t_{k+1} - t_k > 0$ be the fixed step size. Let $R_k \in \mathrm{SO}(3)$ denote the attitude of the rigid body at time t_k. The kinematic equation $\dot{R} = R\Omega^{\times}$ can be approximated as

$$R_{k+1} = R_k F_k, \quad \text{where} \quad F_k = \exp(h\Omega^{\times}) \approx \mathbb{I} + h\Omega_k^{\times}. \tag{8.5}$$

This approximation is based on the assumption that the angular velocity Ω_k is constant in the time interval $[t_k, t_{k+1}]$. Also, note that the discretization scheme is locally second order in h on $\mathrm{SO}(3)$.

For the time interval $[t_k, t_{k+1}]$, the first term in Eq. (8.4) can be approximated as

$$\int_{t_k}^{t_{k+1}} \mathcal{L}(R(t), \Omega(t))dt \approx h\mathcal{L}_d(R_k, \Omega_k), \tag{8.6}$$

where $\mathcal{L}_d$ denotes the discrete Lagrangian. The second term in Eq. (8.4) is approximated as

$$\int_{t_k}^{t_{k+1}} \langle \tau^{\times}(R(t), \Omega(t)), \Sigma^{\times} \rangle dt \approx \frac{h}{2} \langle \tau^{\times}(R_k, \Omega_k) + \tau^{\times}(R_{k+1}, \Omega_k), \Sigma_{k+1}^{\times} \rangle. \tag{8.7}$$

So, the *discrete Lagrange-d'Alembert Principle* is given by

$$\delta \sum_{k=0}^{N-1} \mathcal{L}_d(R_k, \Omega_k) + \frac{1}{2} \sum_{k=0}^{N-1} \langle \tau^{\times}(R_k, \Omega_k) + \tau^{\times}(R_{k+1}, \Omega_k), \Sigma_{k+1}^{\times} \rangle = 0, \tag{8.8}$$

where $\delta R_k = R_k \Sigma_k^{\times}$ and $\Sigma_0 = \Sigma_N = 0$. Equation (8.8) is utilized to obtain a Lie group variational integrator for the feedback attitude dynamics of an AUV. We discuss this step in detail in the next section.

8.2.2 Discrete Equations of Motion

We obtain a Lie group variational integrator as a discrete version of the feedback-controlled rigid body attitude dynamics, based on the discrete Lagrange-d'Alembert principle. The integrator obtained is different from those obtained in [34] - [35] in the sense that in our case the rigid body dynamics model has non-conservative feedback control torques that are not obtained from an optimal control scheme. One can find a detailed description on discretizing *Hamilton's principle* and the Lagrange-d'Alembert principle for mechanical systems in [23] and [42].

In [34], the authors have compared the results obtained from the Lie Group variational integrator with the RK method to demonstrate that the variational integrator exhibits characteristic, symplectic and momentum preservation properties, as well as good energy behavior characteristics of variational integrators. The variational method also preserves the orthogonal structure of $\mathrm{SO}(3)$ without need for reprojection. In this thesis, we extend

this approach to incorporate time-varying control moments that depend on attitude and angular velocity using the discrete Lagrange-d'Alembert principle given in Eq. (8.8).

In [47], the author has obtained a Lie group variational integrator for the feedback attitude dynamics of a spacecraft in the presence of non-conservative, time-varying potential and external moments. Deriving the equations similarly to [47], the Lie group variational integrator can be described by the following discrete time equations

$$F_k\mathcal{J} - \mathcal{J}F_k^T = h(J\Omega_k)^\times, \tag{8.9}$$

$$R_{k+1} = R_k F_k, \tag{8.10}$$

$$J\Omega_{k+1} = F_k^T J\Omega_k + hM_b(R_k) + \frac{h}{2}(\tau_k^- + \tau_k^+), \tag{8.11}$$

where $\tau_k^- = \tau(R_k, \Omega_k)$ and $\tau_k^+ = \tau(R_{k+1}, \Omega_k)$. The integrator yields a map $(R_k, \Omega_k) \mapsto (R_{k+1}, \Omega_{k+1})$ by solving the implicit Eq. (8.9) to obtain F_k and substituting it into Eqs. (8.10) and (8.11) to obtain R_{k+1} and Ω_{k+1}. A method to solve the implicit Eq. (8.9) using Newton iterations is given in [34], [48].

Chapter 9
Simulation Results: Trajectory Tracking in $\mathbf{SO(3)}$

In this chapter, we discuss the results obtained by simulating the feedback dynamics discussed in Chapter 4. The feedback attitude dynamics in $\mathrm{SO}(3)$ are simulated by two different numerical schemes: using a Lie group variational integrator and using a RK-CG scheme.

9.1 Variational Integration of the Feedback Attitude Dynamics

The variational approach was discussed in detail in Section 8.2. In this section, we present some numerical simulation results obtained from applying the Lie Group variational integrator presented in Eqs. (8.9)-(8.11) to the feedback-dynamics of an AUV given in Chapter 4.

9.1.1 Simulation Results and Observations

The parameters used in the variational integration scheme are those of ODIN. A detailed list of the various physical as well as hydrodynamic parameters of ODIN can be found in [50]. These parameters are given in Table 1.

The gain values appearing in the feedback control law are taken to be

$$L = \text{diag}([3.3 \quad 1.4 \quad 2.1]), \quad K = 2.1\text{diag}([1 \quad 2 \quad 3]), \quad \text{and} \quad \Phi(x) = 7x.$$

The attitude time trajectory to be tracked is given by

$$R_r(t) = \begin{bmatrix} c_\theta c_\psi & s_\phi s_\theta c_\psi - c_\phi s_\psi & c_\phi s_\theta c_\psi + s_\phi s_\psi \\ c_\theta s_\psi & s_\phi s_\theta s_\psi + c_\phi c_\psi & c_\phi s_\theta s_\psi - s_\phi c_\psi \\ -s_\theta & c_\theta s_\phi & c_\theta c_\phi \end{bmatrix},$$

where $c_\alpha = \cos(\alpha(t))$ and $s_\alpha = \sin(\alpha(t))$. This attitude profile is obtained from a (1,2,3)-Euler angle representation with $\phi(t) = 0.003t - 0.5, \quad \theta(t) = 0.004t - 0.9, \quad$ and $\quad \psi(t) = 0.001t + 0.9$. Thus, the desired angular velocity, described in the body reference frame, is given by

$$\Omega_r(t) = \begin{bmatrix} \dot{\phi} - \dot{\psi} s_\theta \\ \dot{\theta} c_\phi + \dot{\psi} c_\theta s_\phi \\ -\dot{\theta} s_\phi + \dot{\psi} c_\theta c_\phi \end{bmatrix}.$$

Mass	123.8 kg	$B = \rho g \mathcal{V}$	1215.8 N	C_B	$(0, 0, -7)^T$ mm
Diameter	0.64 m	$W = mg$	1214.5 N	C_G	$(0, 0, 0)^T$ mm
$M_f^{\nu_1}$	70 kg	$M_f^{\nu_2}$	70 kg	$M_f^{\nu_3}$	70 kg
I_{xx}	5.46 kg m^2	I_{yy}	5.29 kg m^2	I_{zz}	5.72 kg m^2
$J_f^{\Omega_1}$	0 kg m^2	$J_f^{\Omega_2}$	0 kg m^2	$J_f^{\Omega_3}$	0 kg m^2

Table 1: Main dimensions and hydrodynamics parameters of ODIN

Note that the angular rates are constant. Whence, $\dot{\Omega}_r(t)$ can be easily obtained from $\Omega_r(t)$ as

$$\dot{\Omega}_r(t) = \begin{bmatrix} -c_\theta \dot{\psi}\dot{\theta} \\ -s_\phi \dot{\theta}\dot{\phi} - s_\theta s_\phi \dot{\psi}\dot{\theta} + c_\theta c_\phi \dot{\psi}\dot{\phi} \\ -c_\phi \dot{\theta}\dot{\phi} - s_\theta c_\phi \dot{\psi}\dot{\theta} - c_\theta s_\phi \dot{\psi}\dot{\phi} \end{bmatrix}.$$

With these simulation parameters for ODIN, we implement the Lie group variational integrator given in Eqs. (8.9)-(8.11) with the dynamic model of Eq. (4.3), error dynamics model Eq. (4.7) and control law Eq. (4.8). We assume the following initial tracking errors

$$Q(0) = \begin{bmatrix} 0.9567 & -0.2863 & 0.0524 \\ 0.1063 & 0.5115 & 0.8527 \\ -0.2709 & -0.8102 & 0.5198 \end{bmatrix}, \qquad \omega(0) = \begin{bmatrix} 0.0252 \\ -0.0189 \\ 0.0147 \end{bmatrix}.$$

Next, we give the numerical simulation results with a time step size of $h = 0.01$ seconds. The final time is taken to be $T = 600$ secs.

The plotted results are the norm of the attitude tracking error, the norm of the angular velocity tracking error and the norm of the control torque. The attitude error norm is defined as $\|\zeta(t)\|$ where $Q(t) = \exp(\zeta^\times(t))$.

A plot of the norm of the attitude tracking error is given in Fig. 1. Figure 2 presents a plot of the norm of the angular velocity tracking error. A plot of the norm of the control moment is given in Fig. 3. The time scale in these plots is normalized by dividing t by the

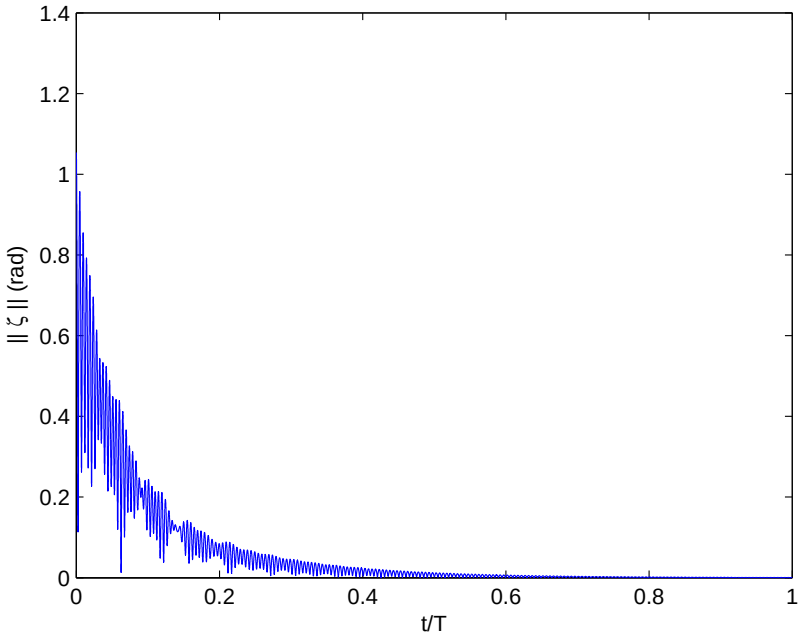

Figure 1: Evolution of attitude tracking error norm under LGVI scheme.

final time $T = 600$ s in the simulated motion.

From Fig. 1 and Fig. 2, we see that the tracking error asymptotically decreases to zero. This validates the asymptotic tracking properties of the control law given in Chapter 4. The norm of the control moment, as shown in Fig. 3 decreases asymptotically.

In the next section, we compare these results with the simulation results obtained using a RK-CG numerical scheme.

9.2 RK-CG Integration of the Feedback Attitude Dynamics

In Chapter 8, we discussed the CG scheme for solving a differential equation on a matrix Lie group. The attitude error kinematics of the AUV given by Eq. (4.6) is an example

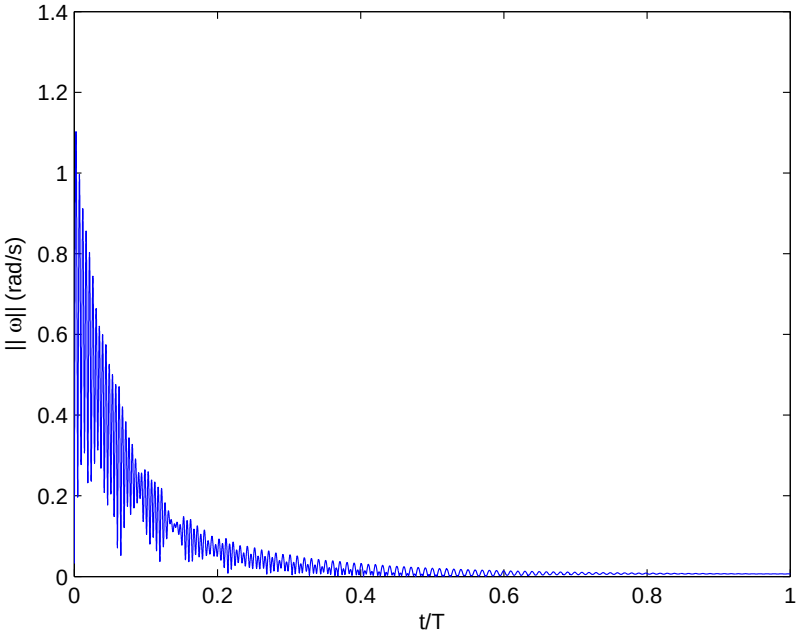

Figure 2: Evolution of angular velocity tracking error norm under LGVI scheme.

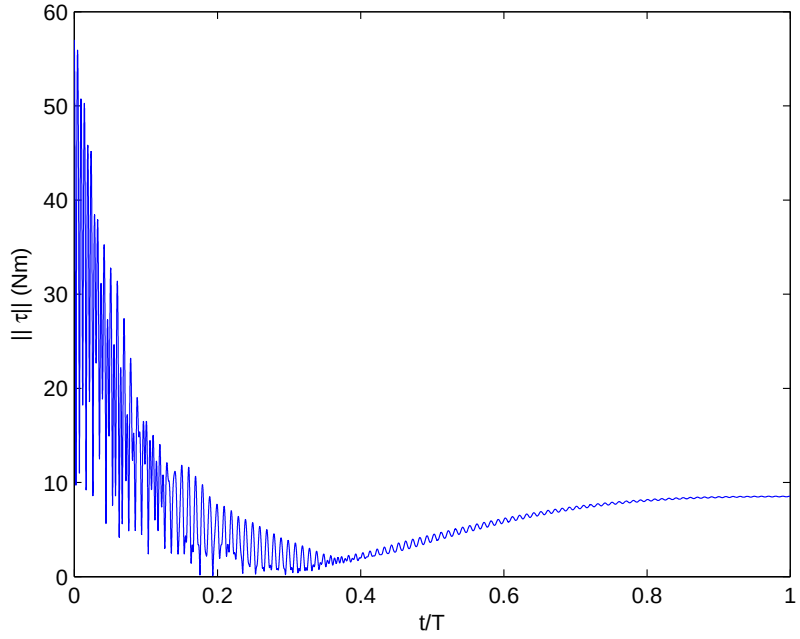

Figure 3: Evolution of norm of control torque under LGVI scheme.

of such a differential equation. We solve Eq. (4.6) using the CG method. Runge-Kutta method is used to solve the attitude error dynamics given by Eq. (4.7) together with the control law in Eq. (4.8).

The algorithm used to integrate the feedback-controlled attitude dynamics in Eqs. (4.6)-(4.8) is as follows: let i be the present time step. Using the attitude error Q_{i-1}, and the angular velocity tracking error ω_{i-1} from the previous step, we calculate τ_i from Eq. (4.8). We use τ_i to solve Eq. (4.7) by RK method and obtain ω_i. Then, ω_{i-1} and ω_i are used to obtain Q_i from Eq. (4.6) using CG scheme.

In the next section, we present the simulation results obtained from a numerical scheme based on the above algorithm.

9.2.1 Simulation Results and Observations

The simulation parameters for this method is the same as that given in Section 9.1.1 for the variational method. The time step size is again taken to be $h = 0.01$ s and the total simulated time is $T = 600$ s.

The plot of the norm of the attitude tracking error is given in Fig. 4. Figure 5 gives the plot of the norm of the angular velocity tracking error. The plot of the norm of the control moment is given in Fig. 6.

The attitude error norms, attitude tracking error norm Fig. 4 and the angular velocity tracking error norm Fig. 5, decrease asymptotically with time.

Comparing Fig. 1 and Fig. 4, we see that the attitude error norm shows similar decreas-

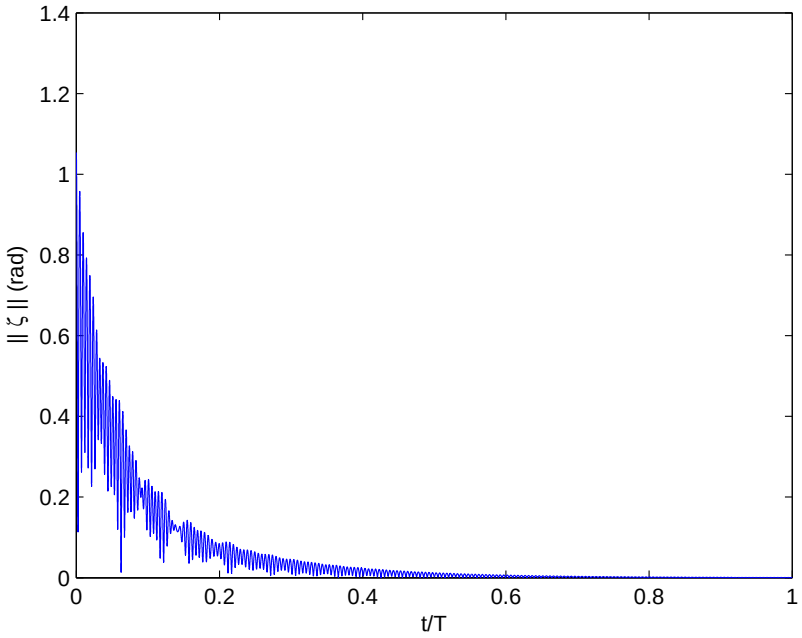

Figure 4: Evolution of attitude tracking error norm under RK-CG scheme.

ing pattern in both of the integration schemes. In Fig. 2 and Fig. 5 we observe that both display an assymptotic decrease in the angular velocity tracking error. However, the final angular velocity tracking error shown in Fig. 5 is less than that shown in Fig. 2. Comparing Fig. 3 and Fig. 6, we observe that the norm of the control torque follows a similar pattern in both the cases.

As mentioned earlier, the Lie group variational integrator exhibits characteristic symplectic and momentum preservation properties, as well as good energy behavior characteristics of variational integrators. Successful application of the variational integrators for the feedback control of the attitude dynamics of an AUV motivates us to extend it to the feedback tracking problem in $\mathrm{SE}(3)$, which can be investigated in the future.

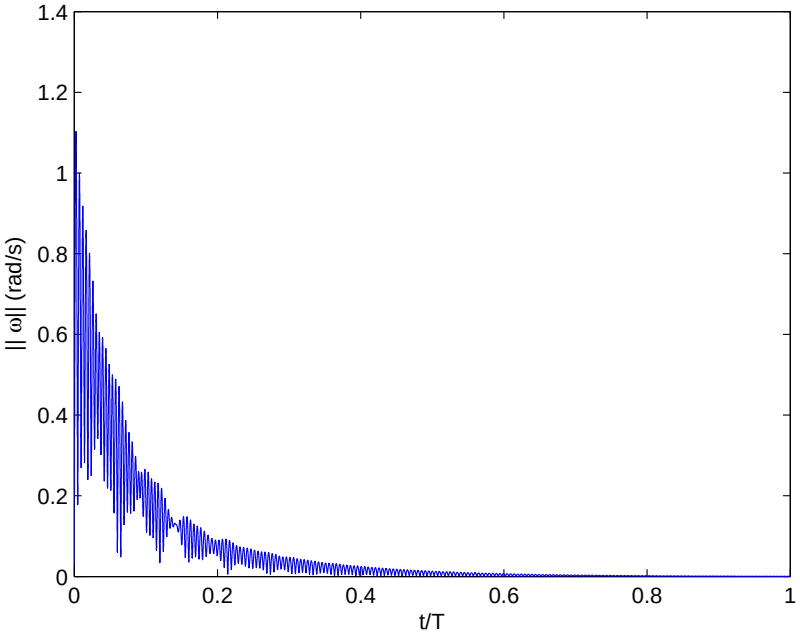

Figure 5: Evolution of angular velocity tracking error norm under RK-CG scheme.

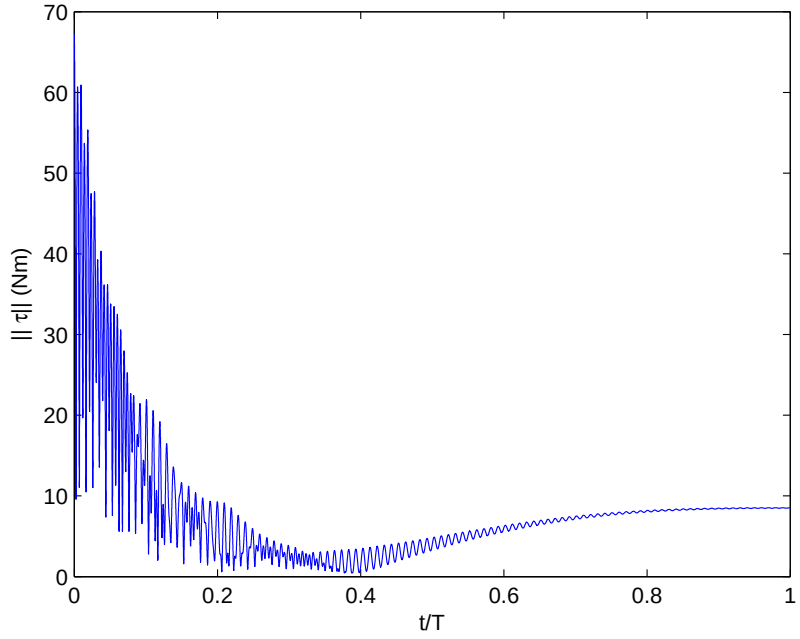

Figure 6: Evolution of norm of control torque under RK-CG scheme.

Chapter 10
Simulation Results: Trajectory Tracking in $\mathbf{SE(3)}$

For simulating the feedback dynamics in $\mathrm{SE}(3)$, we use a Crouch-Grossmann integrator (see [23]) for attitude motion and a fourth-order Runge-Kutta scheme for translational motion.

10.1 Feedback Trajectory Tracking in $\mathrm{SE}(3)$

In this section, we present the numerical simulation results obtained from applying the RK-CG numerical integration scheme to the feedback attitude dynamics given in Chapter 5. As mentioned before, we use published hydrodynamic parameters and other physical parameters of ODIN for our simulation. These parameters are given in Table 1.

For our purpose we take the drag forces and moments matrix acting on ODIN to be $\mathrm{diag}(D_1,\ D_2,\ D_3,\ D_4,\ D_5,\ D_6) = \mathrm{diag}(-231, -231, -120, -37.2, -37.2, -28.57)$. In [50], the author has painstakingly calculated the drag forces and moments acting on ODIN during the experiments examined in this thesis.

In Chapter 7, we discuss in detail the method employed to generate the reference trajectories. We use the feedback control scheme developed in Chapter 5 to track the desired trajectories with an initial error in the states. In [50], the author has implemented open-loop control schemes for different mission scenarios for ODIN. For our numerical

simulations, we pick three of these mission scenarios so that we can validate our feedback control scheme. For each mission, we use the open-loop control, calculated in [50], to solve the system of equations given in Lemma 3.1, using fourth-order RK numerical integrator. Thus for the feedback control simulations, we get the desired trajectory given by translational and angular velocities, given by $\nu_r(k)$ and $\Omega_r(k)$, respectively at discrete time steps (see Chapter 5). Once we get the desired velocities, we can use the equations from Lemma 3.1 again to get the desired translational and angular accelerations, given by $\dot{\nu}_r(k)$ and $\dot{\Omega}_r(k)$, respectively at discrete time steps.

Now, we are ready to simulate the feedback error dynamics given by Eqs. (5.3), (5.4), (5.5), (5.7) and (5.8). The initial error in attitude, $Q(0)$ is taken to be the same as the one given in Section 9.1.1. The error in inertial position at time $t = 0$ is $a(0) = [0.07 \quad 0.08 \quad 0.09]^T$ m. The initial errors in the translational and angular velocity measured in the body-fixed frame are $\upsilon(0) = 0.5[0.06 \quad 0.08 \quad 0.09]^T$ m/s and $\omega(0) = 2.1[0.12 \quad -0.09 \quad 0.07]^T$ rad/s respectively.

The algorithm used to numerically simulate the feedback-controlled dynamics is as follows: let i be the present time step. Using the errors $x_{i-1}, Q_{i-1}, \upsilon_{i-1}$, and$\omega_{i-1}$, we calculate the control forces and moments, φ_i and τ_i using Eqs. (5.4) and (5.5). The feedback control force and moment, φ_i and τ_i is then used in Eqs. (5.4) and (5.5) to obtain υ_i and ω_i. We use RK numerical scheme to perform this simulation. We also calculate x_i in the same routine. Then ω_{i-1} and ω_i are used to obtain Q_i from Eq. (5.3) using a CG scheme. For all the missions, the time step size for numerical integration is $h = 0.01$ s.

This algorithm is repeated for $0 \leq t \leq T$. In the next section, we present the simulation

results for the different mission scenarios obtained from a numerical scheme based on the above algorithm.

As a motivation for the use of feedback control, we present the simulation results for a scenario when the vehicle has to perform a desired mission in the presence of initial disturbances without a feedback loop. This is achieved by integrating the system of equations given in Lemma 3.1 using fourth-order RK method. The initial value of the states for this integration is given by $[b_1(0),\ b_2(0),\ b_3(0),\ \phi(0),\ \theta(0),\ \psi(0),\ \nu_1(0),\ \nu_2(0),\ \nu_3(0), \Omega_1(0),\ \Omega_2(0),\ \Omega_3(0)]$=[$0.07$m, 0.08m, 0.09m, -1.0004rad, 0.2743rad, 0.1107rad, 0.03m/s, 0.04m/s, 0.045m/s, 0.252rad/s, -0.189rad/s, 0.147rad/s]. Note that these initial values corresponds to the initial errors discussed above.

10.1.1 Mission 1

In this mission the AUV is expected to perform a pure body-heave motion of 2.5 m . The trajectory lasts for 8 seconds.

Before we give the simulations results for the feedback control scheme, let us plot the trajectory of the AUV, in the presence of initial disturbances, under an open-loop control scheme. In Fig. 7, we plot the translational and angular positions of the vehicle. Figure 8 gives the open-loop control forces (σ) and moments (τ).

From Fig. 7 we observe that the final position of the vehicle is not what was desired. There is a large error in the translational and angular position of the vehicle. This deviations motivates the use of feedback control to track the desired trajectory.

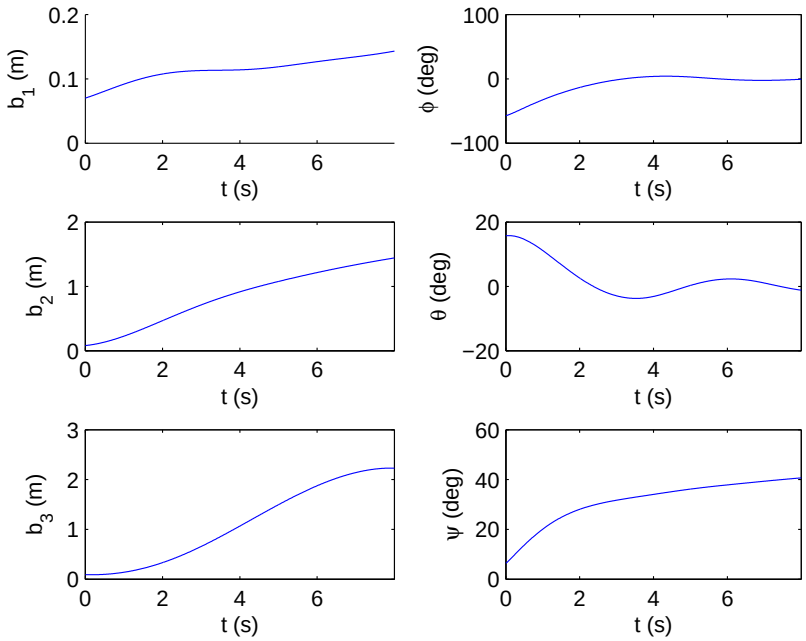

Figure 7: Translational and angular positions using open-loop control with initial disturbances (Mission 1).

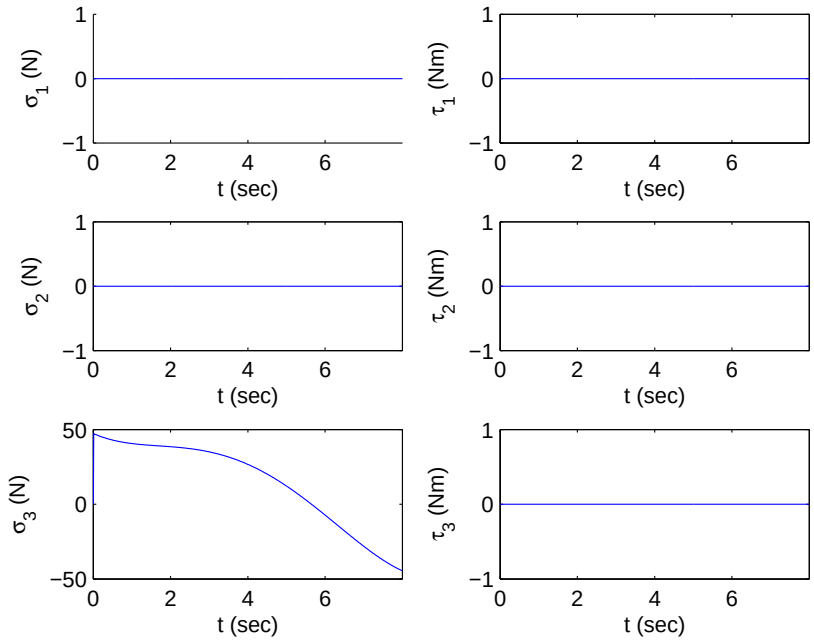

Figure 8: Open loop-controls (Mission 1).

Next, we present the simulation results obtained using feedback control. Note that in this case, the reference trajectory has been generated using the fact that the initial states are zero. The control parameters for this simulation are taken to be (see Chapter 5)

$L_\nu = 4\ \textit{diag}([20,\ 30,\ 40]), \quad L_\Omega = 5\ \textit{diag}([4.4,\ 5.5,\ 6.6]), \quad N = 8\ \textit{diag}([22,\ 26,\ 50]),$ and $K = 1.2\ \textit{diag}([1,\ 2,\ 3]).$

The evolution of the position of the AUV with time is plotted in Fig. 9. In Fig. 10, we compare the actual velocities of the AUV with the reference velocities. From Fig. 10 we see that the errors in the velocities in the six degrees of freedom of the AUV decrease as time progresses. Figures 9 and 10 show an exceptional performance of the controller to track the desired trajectory. We see that the feedback control corrects the initial error in the states and the final position of the vehicle matches well with its desired state. In spite of the presence of initial disturbances, the vehicle is able to realize a pure heave motion of 2.5 m. In Fig. 11 we compare the control effort required for the feedback scheme, in the presence of initial errors, as compared to the open-loop control scheme with no initial disturbances.

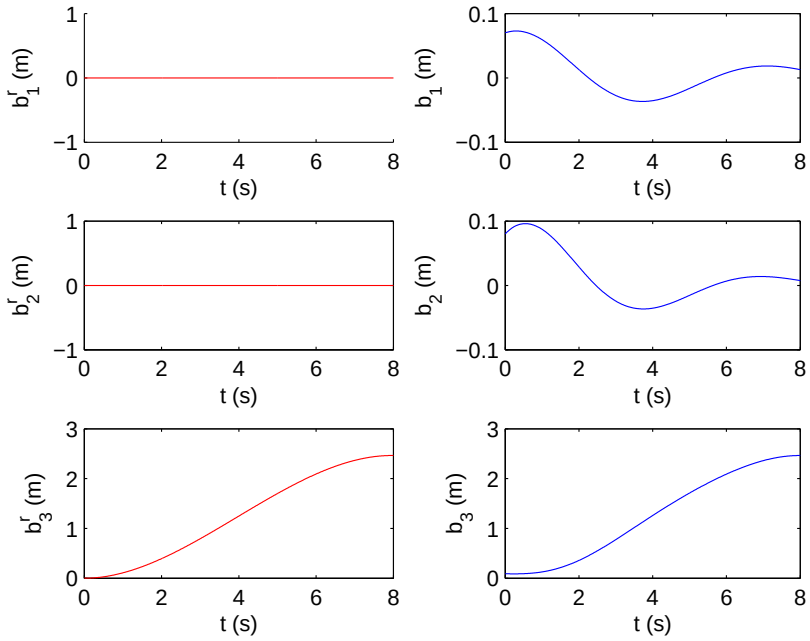

Figure 9: Comparison of the reference(b_j^r) and actual(b_j) position of the AUV (Mission 1).

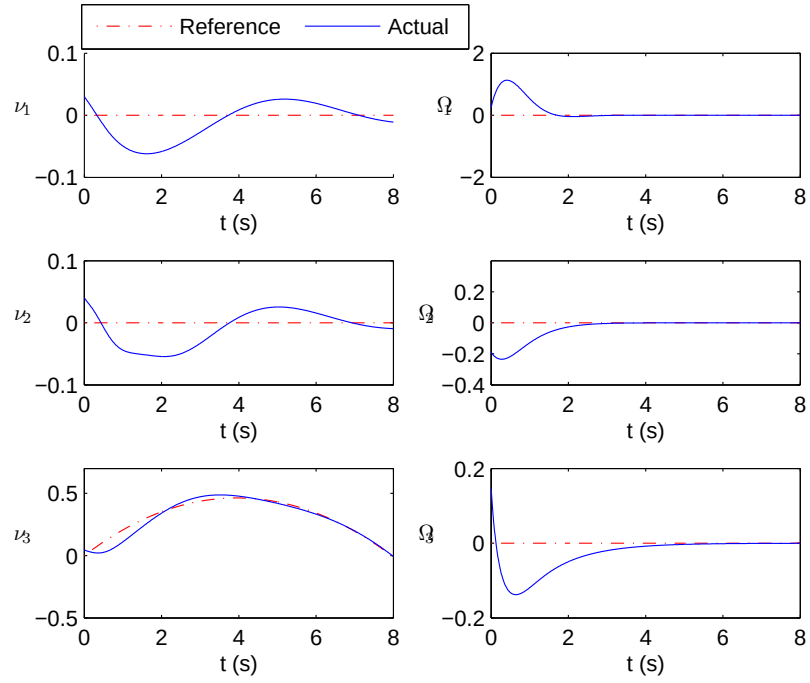

Figure 10: Comparison of the reference and actual velocities of the AUV (Mission 1).

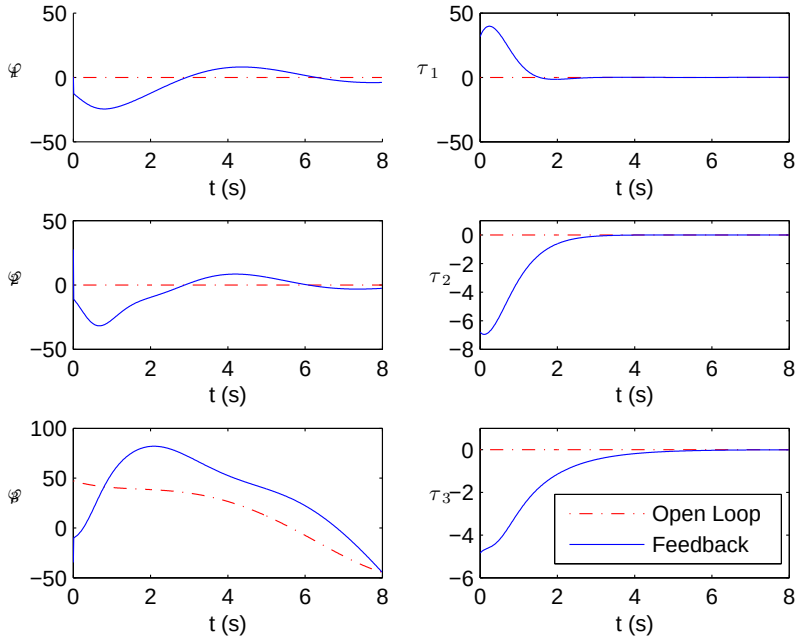

Figure 11: Comparison of the control effort in feedback scheme as compared to the open-loop scheme (Mission 1).

10.1.2 Mission 2

For this mission the AUV is expected to perform a positive pure surge (i.e. motion in b_1-direction) of 5 m. This mission lasts for 30 sec.

First of all let us plot the trajectory of the AUV in the presence of initial disturbances, under open loop control scheme. In Fig. 12, we plot the translational and angular positions of the vehicle. Figure 13 gives the open loop control forces and moments.

From Fig. 12 we observe that the there is a large error in the translational and angular position of the vehicle. As a result of coupling between yaw angle and sway, the error

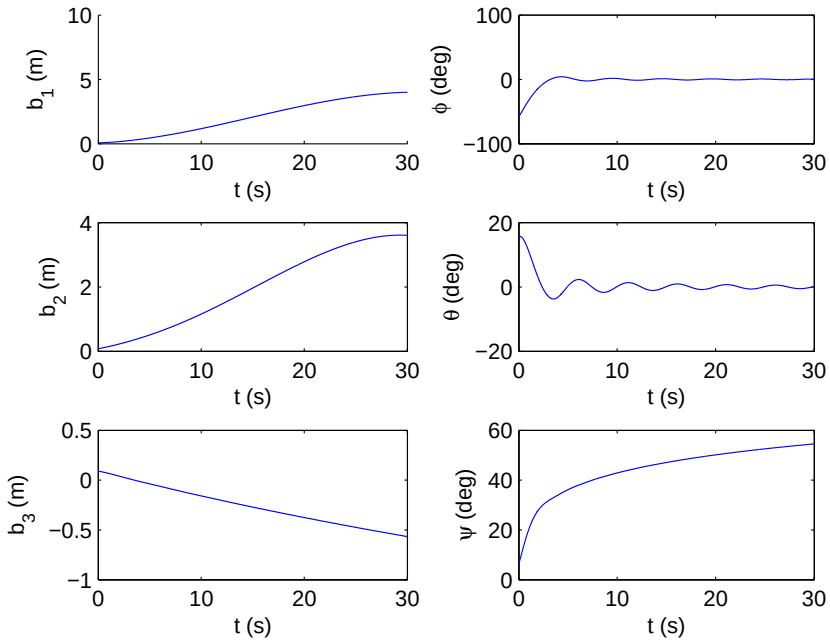

Figure 12: Translational and angular positions using open-loop control with initial disturbances (Mission 2).

in yaw angle shows up in the sway motion of the vehicle. Since the control moment is zero (see Fig. 13), the roll angle of the vehicle goes to zero as time progresses. We also observe a change in the depth of the vehicle with time. As pitch angle and heave motion are coupled, we see an error in the pitch angle as well.

Now let us plot the simulation results obtained using feedback control scheme. Note that the reference trajectories were generated using open-loop control scheme in the absence of initial disturbances. The control parameters for this simulation are $L_\nu = 0.5\,\textit{diag}([10\ 10\ 10])$, $L_\Omega = 5\,\textit{diag}([4.4\ 5.5\ 6.6])$, $N = 0.5\,\textit{diag}([12\ 12\ 12])$, *and* $K = 1.2\,\textit{diag}([1\ 2\ 3])$.

Figure 14 plots the reference trajectory and the actual trajectory. In Fig. 15 we give the evolution of the desired and the actual Euler angles with time. A comparison of the

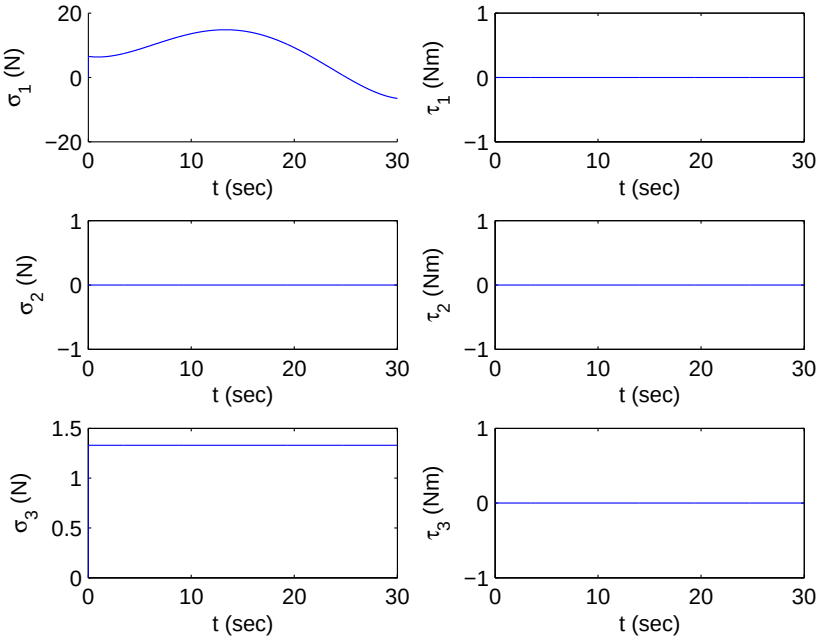

Figure 13: Open-loop controls (Mission 2).

reference and the actual velocities of the AUV is made in Fig. 16. The control effort for both the feedback and open-loop control scheme is plotted in Fig. 17. It is evident from Figs. 14, 15 and 16 that the controller tracks the desired trajectory quite well.

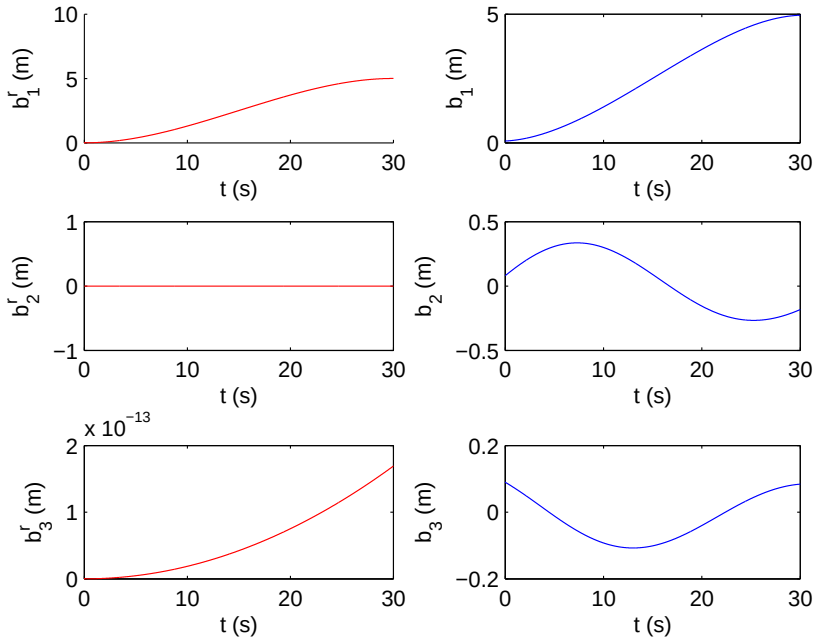

Figure 14: Comparison of the reference(b_j^r) and actual(b_j) position of the AUV, (Mission 2).

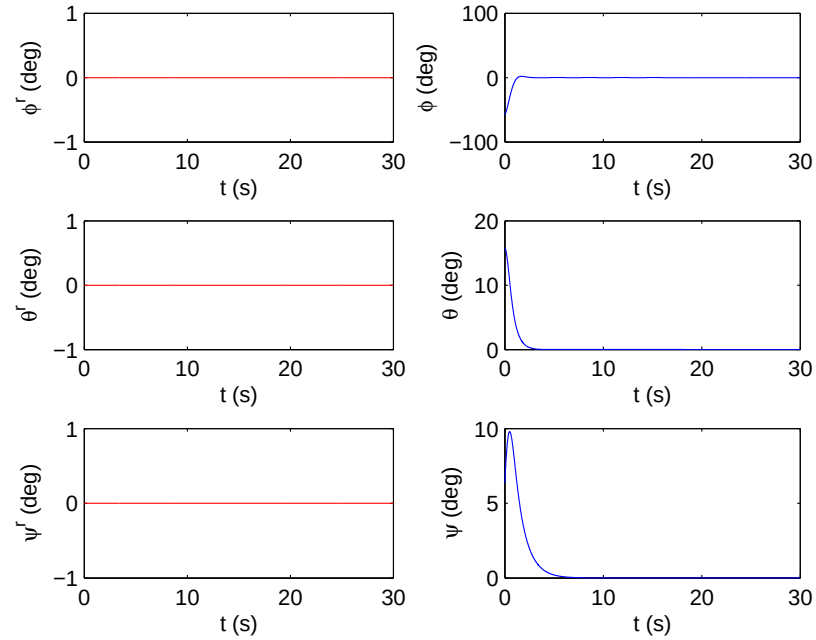

Figure 15: Comparison of the reference $(\cdot)^r$ and actual Euler angles of the AUV, (Mission 2).

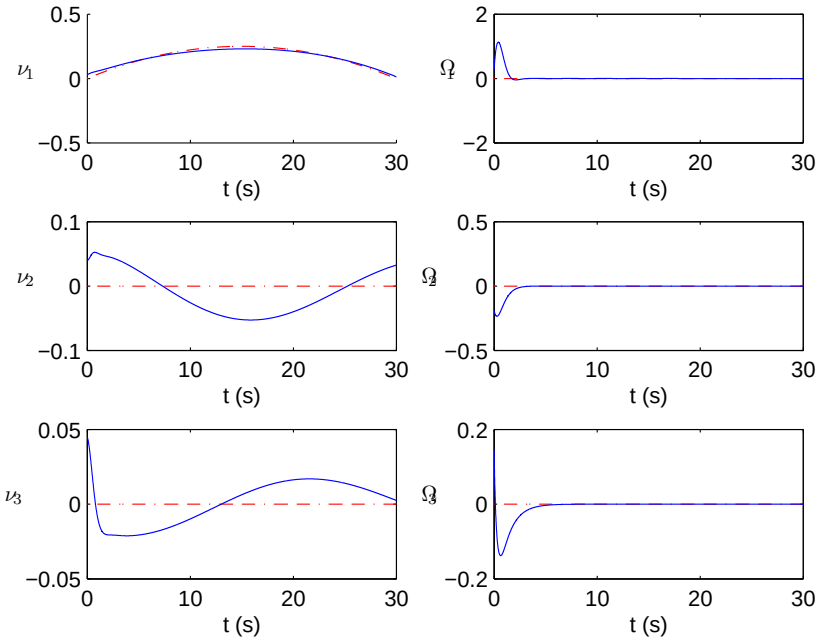

Figure 16: Comparison of the reference and actual velocities of the AUV (Mission 2).

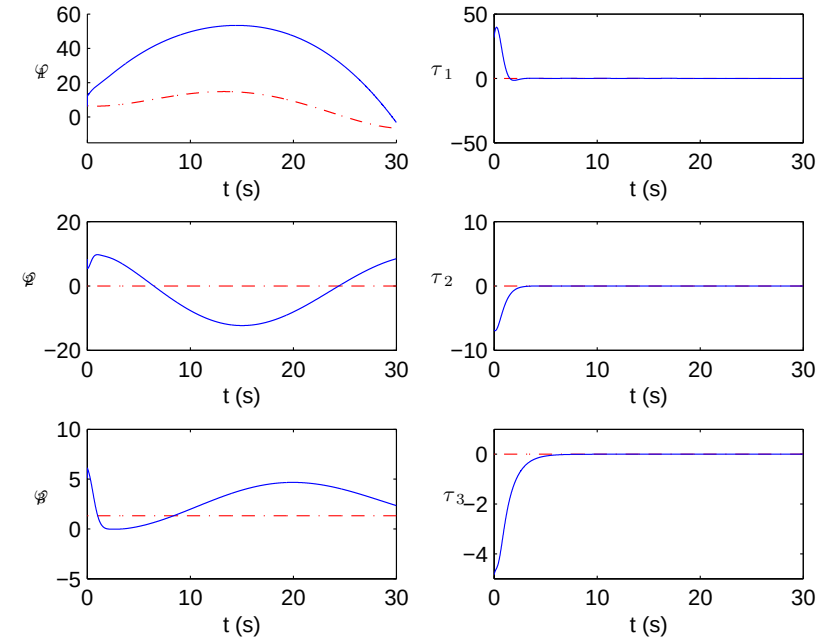

Figure 17: Comparison of the control effort in feedback scheme as compared to the open-loop scheme (Mission 2).

10.1.3 Mission 3

For this mission the AUV has to execute a more complex trajectory. In [50], the design of this trajectory was motivated by the practical use of AUV to perform a seabed survey. Assuming that a camera is fit at its front, the AUV is expected to perform an L-shaped motion while maintaining a constant pitch angle of $\theta = -20^\circ$ and constant depth throughout its motion. The vehicle executes this trajectory in three separate stages. For the first 5 seconds, the vehicle stabilizes at a pitch angle of $\theta = -20^\circ$. In the second leg of its motion, from $t = 5$ to 35 s, the vehicle has to move 5 m in the positive surge direction (i.e., in positive b_1-direction) while maintaining a constant depth and a constant pitch. In the last stage, which spans from $t = 35$ to 47 s, the vehicle has to move 2 m in the positive sway direction (i.e., positive b_2-direction) while maintaining the same depth and pitch angle. We assume the buoyant force acting on the vehicle to be $B = 0.82 + W$.

At first we plot the trajectory of the AUV in the presence of initial disturbances, under open loop control scheme. In fig 18, we plot the translational and angular positions of the vehicle. Figure 19 gives the open loop control forces and moments.

In Fig. 18, we plot the position and orientation of the vehicle of the AUV in the presence of initial disturbances, under an open-loop control scheme. We observe that the vehicle moves 4 m in the positive b_1-direction in the first 35 s, but then moves backward for the remaining time. This motion was not predicted. There is a large error in the yaw angle which also gets reflected in the error in sway. Thus, we see that in the presence of initial

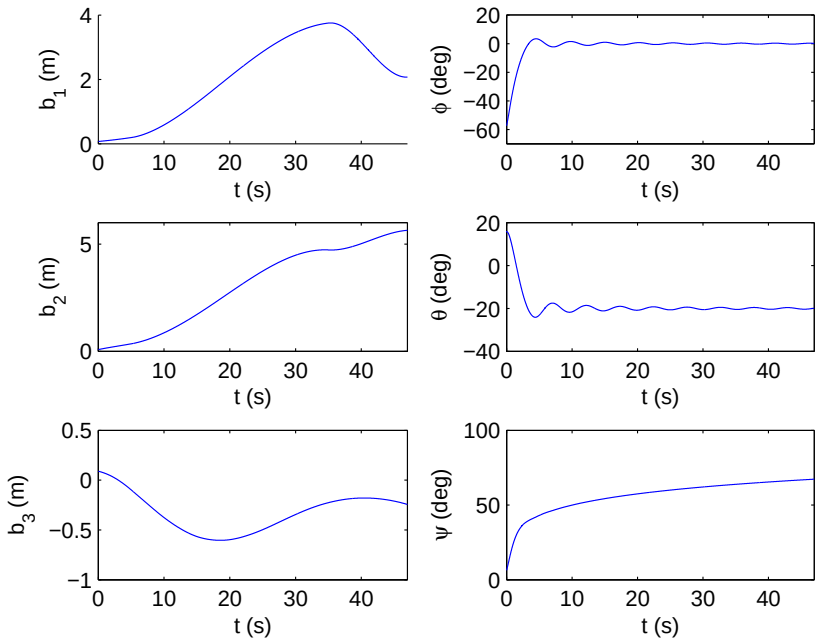

Figure 18: Translational and angular positions using open-loop control with initial disturbances (Mission 3).

disturbances, the desired trajectory is not achieved using an open-loop control scheme. Since a constant moment is applied to hold the pitch angle (see fig 19), we observe that the AUV maintains a constant pitch angle of -20° throughout its motion. Since the control moment is zero in roll direction (see fig 19), the roll angle of the vehicle goes to zero as time progresses. Thus we see that the in the presence of initial disturbances, the desired trajectory is not achieved using open-loop control scheme.

Next, we present the results obtained using a feedback control scheme in the presence of disturbances. The reference trajectory is generated using the open-loop control with the assumption of zero error in the initial states. The control parameters for this simulation are taken as $L_\nu = 0.5\ \textit{diag}([10\ 10\ 10])$, $L_\Omega = 5\ \textit{diag}([4.4\ 5.5\ 6.6])$, $N =$

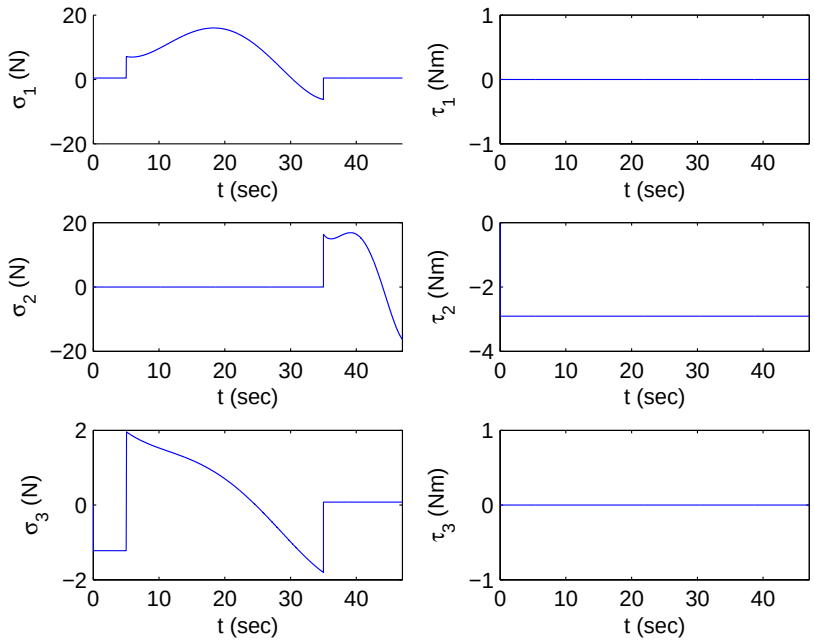

Figure 19: Open-loop controls (Mission 3).

0.5 *diag*$([12\ 12\ 12])$, *and* $K = 1.2$ *diag*$([1\ 2\ 3])$. Figure 20 plots the reference trajectory and the actual trajectory. In Fig. 21 we give the evolution of the desired and the actual Euler angles with time. A comparison of the reference and the actual velocities of the AUV is made in Fig. 22. The control effort for both the feedback and open-loop control scheme is plotted in Fig. 23. In Fig. 20 we notice that the feedback controller tracks the desired trajectory quite well. We observe from the reference plots that for the first 5 s, the vehicle does not move in the b_1, b_2 or b_3 direction, as was expected. From $t = 5$ to $t = 35$ s, the AUV moves 5 m in the positive surge direction. We also observe from the plot that after $t = 35$ s, the AUV is executing a pure sway motion. In Fig. 21, we see that despite initial errors in the Euler angles, the AUV is able to maintain the -20° pitch angle. The errors in roll and yaw also show an asymptotic decrease.

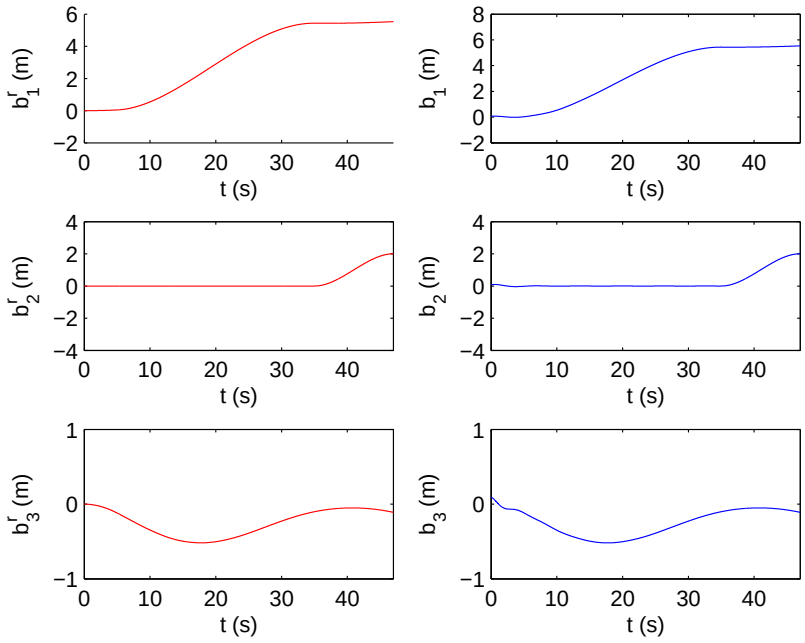

Figure 20: Comparison of the reference(b_j^r) and actual(b_j) position of the AUV, (Mission 3).

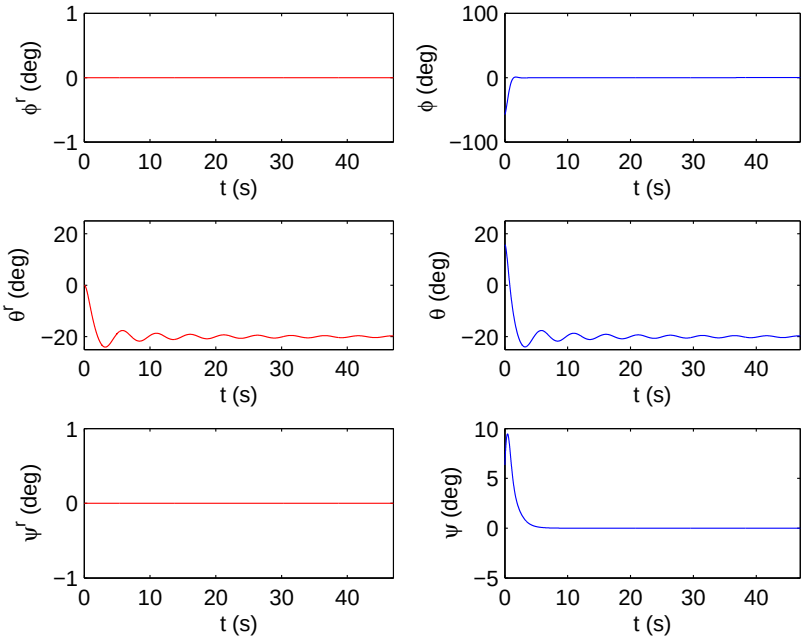

Figure 21: Comparison of the reference $(\cdot)^r$ and actual Euler angles of the AUV, (Mission 3).

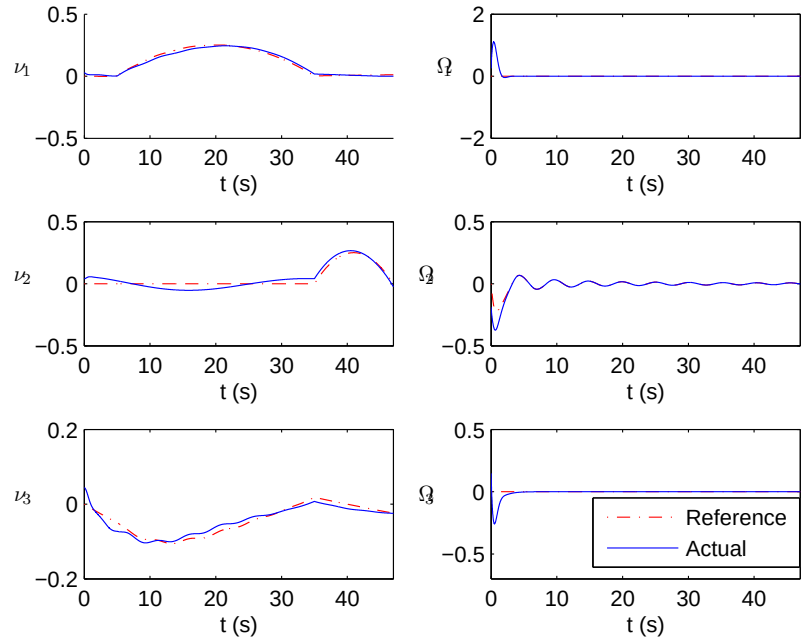

Figure 22: Comparison of the reference and actual velocities of the AUV (Mission 3).

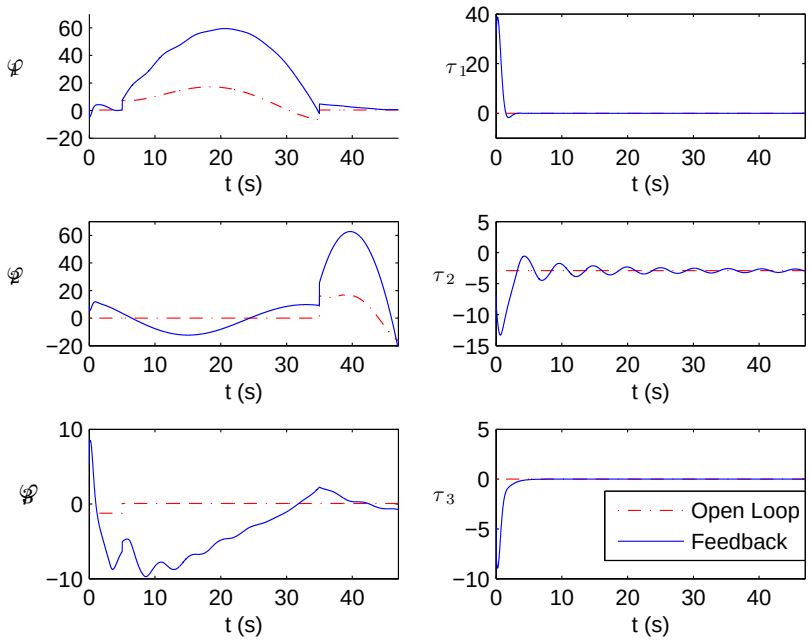

Figure 23: Comparison of the control effort in feedback scheme as compared to the open-loop scheme (Mission 3).

Chapter 11
Conclusions and Future Work

The successful implementation of a feedback control scheme for the attitude dynamics problem in $\mathrm{SO}(3)$ has provided motivation to work with the more general problem in $\mathrm{SE}(3)$. The main outcome of this research is that by using a feedback control scheme, we can attenuate the effect of initial disturbance forces and moments on the dynamics of the AUV. This will help us in our endeavor to test motion planning algorithms on an AUV in the uncertain environment of the oceans.

This thesis opens many doors for possible future work in the area of AUV motion planning and trajectory design. We have demonstrated the ability of a feedback control scheme to track a reference trajectory of an AUV in the presence of initial errors in its states. However, implementing the feedback control scheme on ODIN is the next major challenge. First and foremost, it will require an advanced sensor on board the vehicle. Also, as reported in [50], one faces several practical problems while implementing the theoretically designed trajectories on a real vehicle. Such issues have to be dealt with in the future.

In this thesis, we have looked at a scenario where the vehicle experiences disturbance forces at the start of its mission. This may be extended to incorporate bounded and time-varying external disturbances in the dynamics of the vehicle. Thus, a robust feedback controller has to be designed to track the desired trajectory while rejecting the effects of these disturbances. The design of adaptive control schemes for trajectory tracking falls

within the realm of possible future research.

In this thesis, we used a Lie group variational integrator to simulate the feedback controlled attitude dynamics of an AUV. An extension of this method to discretize the feedback dynamics of an AUV in $\mathrm{SE}(3)$ is also an area of future investigation.

References

[1] Allmendinger, E.E., 'Submersible vehicle design', SNAME, 1990.

[2] Antonelli, G., Chiaverini, S., Sarkar, N., & West, M., 'Adaptive control of an autonomous underwater vehicle experimental results on ODIN', IEEE Transactions on Control Systems Technology, Vol. 9, Issue 5, pp. 756-765, 2001.

[3] Bhattacharyya, R., 'Dynamics of marine vehicles', John Wiley & Sons, 1978.

[4] Bloch, A.M., Baillieul, J., Crouch, P.E., & Marsden, J.E., 'Nonholonomic mechanics and control', Vol. 24 of series in Interdisciplinary Applied Mathematics, Springer-Verlag, New York, 2003.

[5] Boothby, W., 'An introduction to differentiable manifolds and Riemannian geometry', No. 125 in Pure and Applied Mathematics, 2^{nd} edition, Academic Press, Inc., Florida, 1986.

[6] Brockett, R., 'Hybrid models for motion control systems', Essays in Control: Perspectives in the Theory and its Applications, Boston, MA, pp. 29-53, 1993.

[7] Bullo, F. & Lewis, A.D., 'Geometric control of mechanical systems', Springer, 2005.

[8] Bullo, F., Leonard, N., & Lewis, A.D., 'Controllability and motion algorithms for underactuated Lagrangian systems on Lie groups' IEEE Transactions on Automatic Control, 45/8, pp. 1437-1454, 2000.

[9] Chaturvedi, N.A., & McClamroch, N.H., 'Almost global attitude stabilization of an orbiting satellite including gravity gradient and control saturation effects', Proceedings of American Control Conference, 2006.

[10] Chyba, M., Haberkorn, T., Smith, R.N., & Choi, S.K., 'Design and implementation of time efficient trajectories for autonomous underwater vehicles', Ocean Engineering, 35/1, pp. 63-76, 2008.

[11] Chyba, M., Haberkorn, T., Smith, R.N., Singh, S., & Choi, S., 'Increasing underwater vehicle autonomy by reducing energy consumption', Ocean Engineering: Special Editions on AUVs, 36/1, pp. 62-73, 2009.

[12] Chyba, M., Haberkorn, T., Smith, R.N., & Wilken, G., 'A geometric analysis of trajectory design for underwater vehicles', Discrete and Continuous Dynamical Systems, Series B, 11/2, 2009.

[13] Chyba, M., & Smith, R.N., 'A first extension of geometric control theory to underwater vehicles', Proceedings of IFAC Workshop on Navigation, Guidance and Control of Underwater Vehicles, Killaloe, Ireland, 2008.

[14] Smith, R.N., Chyba, M., Wilkens, G., & Catone, C., 'A geometric approach to the motion planning problem for a submerged rigid body' International Journal of Control (To Appear).

[15] Craig, J.J., Hsu, P., & Sastry, S., 'Adaptive control of mechanical manipulators', IEEE International Conference on Robotics and Automation, San Franciso, 1986.

[16] Cristi, R., Papoulias, F.A. & Healey, A.J., 'Adaptive sliding mode control of autonomous underwater vehicles in the dive plane', IEEE Journal of Oceanic Engineering, OE, 15/3, pp 152-160, 1990.

[17] Crouch, P.E., & Leite, F.S., 'The dynamic interpolation problem: on Riemannian manifolds, Lie groups, and symmetric spaces', Journal of Dynamic and Control Systems, Vol. 1, pp. 177-202, 1995.

[18] Crouch, P.E., & Grossman, R., 'Numerical integration of ordinary differential equations on manifolds', Journal of Nonlinear Science, Vol. 3, pp. 1-33, 1993.

[19] Fang, M.C., Hou, C.S., & Luo, J.H., 'On the motions of the underwater remotely operated vehicle with the umbilical cable effect', Ocean Engineering, Vol. 34, pp. 1275-1289, 2007.

[20] Feng, Z., & Allen, R., 'Evaluation of the effects of the communication cable on the dynamics of an underwater flight vehicle', Ocean Engineering, Vol. 31, pp. 1019-1035, 2004.

[21] Fossen, T.I., 'Guidance and control of ocean vehicles', John Wiley & Sons, 1994.

[22] Goldstein, H., 'Classical mechanics', 2^{nd} edition, Addition Wisley, Boston, 1980.

[23] Harier, E., Lubich, C., & Wanner, G., Geometric numerical integration, Springer, Berlin, 2000.

[24] Healey, A.J, & Lienard, D., 'Multivariable sliding mode control on autonomous underwater vehicles', IEEE Journal of Ocean Engineering, OE-18/3, pp.327-339.

[25] Hussein, I., Bloch, A.M., 'Constrained optimal trajectory tracking on the group of rigid body motions', Proceedings of 44^{th} IEEE Conference on Decision and Control, pp. 2152-2157, 2005.

[26] Hussein, I.I., Leok, M., Sanyal, A.K., & Bloch, A.M., 'A discrete variational integrator for optimal control problems on $\mathrm{SO}(3)$', Proceedings of IEEE Conference on Decision and Control, pp. 6636-6641, 2006.

[27] Ishii, K., & Ura, T., 'An adaptive neural-net controller system for an underwater vehicle' Control Engineering Practice, Vol. 8, pp. 177-184, 2000.

[28] Jalving, B., & Storkersen, N., 'The control system of an autonomous underwater vehicle', Proceedings of the Third IEEE Conference on Control Applications, Glaskow, UK, pp 851-856, 1994.

[29] Kamnier, I., Pascoal, A.M., & Silvestre, C.J., & Khargonekar, P.P., 'Control of an underwater vehicle using $\mathscr{H}_\infty$ synthesis', Proceedings of the 30^{th} IEEE Conference on Decision and Control, Brighton, UK, Vol. 3, pp. 2350-2355, 1991.

[30] Khalil, H.K., 'Nonlinear systems', Prentice Hall, Upper Saddle River, NJ, 2002.

[31] Kim, T.W., & Yuh, J., 'A novel neuro-fuzzy controller for autonomous underwater vehicles', Proceedings of the IEEE International Conference on Robotics and Automation, Seol, 2001.

[32] Lamb, H., 'Hydrodynamics', 6^{th} edition, Dover Publications, 1945.

[33] Lee, C.S.G., Wang, J.S., & Yuh, J., 'Self-adaptive neuro-fuzzy systems with fast parameter learning for autonomous underwater vehicle control', Proceedings of IEEE International Conference on Robotics and Automation, Vol. 4, pp. 3861-3866.

[34] Lee, T., Leok, M., & McClamroch, N.H., 'A Lie group variational integrator for the attitude dynamics of a rigid body with applications to the 3D pendulum', Proceedings of IEEE Conference on Control Applications, pp. 962-967, 2005.

[35] Lee, T., Leok, M., & McClamroch, N.H., 'Optimal control of a rigid body using geometrically exact computations on $\mathrm{SE}(3)$', Proceedings of IEEE Conference on Decision and Control, pp. 2710-2715, 2006.

[36] Leonard, N.E., 'Stabilization of steady motions of an underwater vehicle', Proceedings of the 35^{th} IEEE Conference on Decision and Control, pp. 961-966, 1996.

[37] Leonard, N.E., 'Stability of a bottom-heavy underwater vehicle', Automatica, Volume 33, No. 3, pp. 331-346, 1997.

[38] Leonard, N.E., 'Control synthesis and adaptation for an underactuated autonomous underwater vehicle', IEEE Journal of Oceanic Engineering, Vol. 20, No. 3, pp. 211-220, 1995.

[39] Leonard, N.E., 'Periodic forcing, dynamics and control of underactuated spacecraft and underwater vehicles', Proceedings of 34^{th} IEEE Conference on Decision and Control, New Orleans, Louisiana, pp. 3980-3985, 1995.

[40] Lewis, A.D., 'Is it worth learning differential geometric methods for modeling and control of mechanical systems?', Robotica, Vol. 25(6), pp. 765-777, 2007.

[41] Liceaga-Castro, E., & Vander-Molen, G.M.,'Submarine $\mathscr{H}_\infty$ depth control under wave disturbances', IEEE Transactions on Control Systems Technology, 3/3, pp. 338-346, 1995.

[42] Marsden, J.E., & West, M., 'Discrete mechanics and variational integrators', Acta. Numerica, 10, pp. 357-514, 2001.

[43] Marsden, J.E. & Ratiu, T.S., 'Introduction to mechanics and symmetry', Second Edition, Springer-Verlag, New York, 1999.

[44] Milnor, J., 'Morse theory', Princeton University Press, Princeton, NJ, 1963.

[45] Sadeh, N.,& Horowitch, R., 'Stability analysis of an adaptive controller for robotic manipulators', Proceedings of IEEE International Conference on Robotics and Automation, Raleigh, NC, 1987.

[46] Sanyal, A.K., & Chaturvedi, N.A., 'Almost global robust attitude tracking control of spacecraft in gravity', Proceedings AIAA Guidance, Navigation and Control Conference, Honolulu, HI, 2008, AIAA-2008.

[47] Sanyal, A.K., 'Almost global robust attitude tracking for spacecraft in gravity with unknown Drag', AIAA, Journal of Guidance, Navigation, Control and Dynamics, 2008. (submitted)

[48] Sanyal, A.K., Lee, T., Leok, M., & McClamroch, N.H., 'Global optimal attitude estimation using uncertainty ellipsoids', Systems and Control Letters, 57/3, pp. 236-245, 2008.

[49] Slotine, J.J.E, & Li, W., 'Adaptive manipulator control: a case study', Proceedings of IEEE International Conference on Robotics and Automation, pp. 1392-1401, 1987.

[50] Smith, R.N., 'Geometric control theory and its applications to underwater vehicles', PhD thesis, University of Hawaii, Manoa, 2008.

[51] Smith, R.N., Singh, S.B., & Chyba, M., 'Decoupled trajectory planning for a submerged rigid body subject to dissipative and potential forces', Proceedings of the IEEE Region 10 Colloquium and Third International Conference on Industrial and Information Systems, Kharagpur, India, 2008.

[52] Spong, M.W., & Ortega, R., 'On adaptive inverse dynamics control of rigid robots', IEEE Transaction on Automatic Control, AC-35, No. 1, pp. 92-95, 1990.

[53] Vander-Molen, G.M., & Grimble, M.J., '$\mathscr{H}_\infty$ submarine depth and pitch control', Proceedings of the 32^{nd} IEEE Conference on Decision and Control, San Antonio, TX, Vol. 3, pp 2511-2516, 1993.

[54] Venkatachalam, R., Limbert, D.E. & Jalbert, J.C., 'Design and simulation of a crabwise motion controller for the EAVE-EAST submersible', ROV, 1985.

[55] William, S.J., & Marshfiled, W.B., 'A switched $\mathscr{H}_\infty$strategy for control of a submarine', International Conference on Control, Edinburg, UK, Vol. 1, pp. 487-491, 1991.

[56] Yoerger, D.R. & Slotine, J.J.K., 'Nonlinear trajectory control of autonomous underwater vehicles using the sliding methodology', Proceedings of ROV Conference, pp 245-251, 1984.

[57] Yoerger, D.R. & Slotine, J.J.K., 'Robust trajectory control of underwater vehicles', IEEE Journal of Oceanic Engineering, OE-10/4, pp 462-470, 1985.

[58] Yoerger, D.R. & Slotine, J.J.K., 'Adaptive sliding control of an experimental underwater vehicle', Proceedings of IEEE International Conference on Robotics and Automation, Sacraemento, California, pp 2746-2751, 1991.

[59] Yuh, J., 'Design and control of autonomous underwater robots: a survey', Autonomous Robots 8, 7-24, Kluwer Academic Publishers, 2000.

[60] Yuh, J., 'An adaptive and learning control system for underwater robots,' Proceedings of 13^{th} World Congress International Federation of Automatic Control A, pp. 145-150, 1996.

[61] Yuh, J., Nie, J., & Lee, C.S.G., 'Experimental study on adaptive control of underwater robots', Proceedings of the IEEE International Conference on Robotics and Automation, Detroit, 1999.

[62] Zadeh, L.A., 'Soft computing and fuzzy logic', IEEE Software, Vol. 11, No. 6, pp. 48-56, 1994.

[63] Zhao, S., Yuh, J., & Choi, S.K., 'Adaptive DOB control for AUVs', Proceedings of IEEE International Conference on Robotics and Automation, Vol. 5, 2004.